ELSEVIER

Comput. Methods Appl. Mech. Engrg. 126 (1995) 39–66

Computer methods in applied mechanics and engineering

Finite element procedure for solving contact thermoelastoplastic problems at large strains, normal and high pressures

A.V. Idesman[a,*], V.I. Levitas[b]

[a]*V.N. Bakul Institute for Superhard Materials of the Ukrainian Academy of Sciences, 2 Avtozavodskaya, Kiev, 254074, Ukraine*

[b]*Institut für Baumechanic und Numerische Mechanik, Universität Hannover, Appelstraße 9A, 30167, Hannover, Germany*

Received 2 August 1993; revised 23 July 1994

Abstract

The paper presents a finite element (FE) procedure for solving contact thermoelastoplastic problems at large strains. A rigorous derivation of the constitutive relations used and the structure of a tangent stiffness matrix and load vector at arbitrary thermomecanical loading are given. The deformation model [1, 2] is used which is based on the multiplicative decomposition of the total deformation gradient to an elastic, temperature and plastic parts and the generalization of Prandtl–Reuss equations to the case of large strains, high pressures and temperatures. A method is proposed for the generalization of the elastic law at small strains to the case of high pressures which is based on the use of the existence of an elastic potential (hyperelastic material) at large elastic strains.

The algorithms for solving thermoelastoplastic problems at large strains and contact elastic problems at small strains are considered individually and in combination for solving contact thermoelastoplastic problems at large strains. An algorithm for solving thermoelastoplastic problems at large strains is based on a modified method of initial stresses allowing the use of both the constant and the variable tangent stiffness matrices. An algorithm allowing for contact conditions (which are described using a friction surface, in the particular case, the Coulomb's law of friction is considered) involves the simultaneous consideration of an arbitrary number of deformable bodies in contact. The pairs of nodes with the same coordinates are introduced along the interface. Owing to transformation of the set of FEM equations, the contact conditions reduce to the usual boundary conditions in terms of stresses or displacement with iterative redetermination of their types (adhesion, slip, no contact) in each pair of nodes. Optimum variants of combinations of the iterative procedures allowing for plastic flow and contact interaction are studied. Particular problems are solved. An attractive feature of the present approach is the simplicity of allowing for the contact conditions for an arbitrary number of deformable bodies in contact and insignificant modifications of computer program which are necessary for the change from small strains to large ones.

1. Introduction

Main aspects of the construction of numerical procedures of solving contact thermoelastoplastic problems at large strains are as follows: (a) the choice of justified deformation models at large strains including the choice of a deformation measure and its decomposition to an elastic, temperature and plastic parts as well as a correct accounting for finite rotations (satisfying the conditions of invariance with respect to rigid rotations and the choice of type of the objective derivative); (b) the development of computational algorithms which include the transition from a continuous problem to a discrete one, the construction of iterative procedures with a high rate of convergence for the consideration of

* Corresponding author.

0045-7825/95/$09.50
SSDI 0045-7825(95)00757-8

physical, geometrical non-linearity and contact conditions; and (c) efficient implementation of the numerical procedure as software which depends mainly on (a) and (b).

The development of models of thermoelastoplastic behaviour of materials at large strains is elucidated in numerous works [1–12 and other]. Many of them are based on multiplicative decomposition of the total deformation gradient to an elastic and plastic parts, which permits a visual geometric interpretation of strains. Problems of development of numerical algorithms of solution of elastoplastic problems at large strains (with the use of Lagrangian and updated Lagrangian formulations) are considered in [3, 13–23 and other]. In this case, the structure of FE equations (i.e. a tangent stiffness matrix and a load vector) is determined by chosen measures of strains and stresses. Models and algorithms of the accounting for contact interaction are given in [13, 23–31 and other].

The present work introduces one of possible approaches to the development of a FEM procedure for solving contact thermoelastoplastic problems at large strains for isotropic materials and contact friction described using a friction surface (in the particular case, the Coulomb's law of friction is considered). The deformation model [1, 2] is used which is based on the multiplicative decomposition of the total deformation gradient to an elastic, temperature and plastic parts and the generalization of Prandtl–Reuss equations to the case of large strains, high pressures and temperatures. And it is supposed that at normal pressures elastic strains are small, at high pressures shear elastic strains are small, while volumetric elastic strains are finite (plastic strains are finite in both cases). A method is proposed for the generalization of the elastic law at small strains to the case of high pressures which is based on the use of the existence of an elastic potential (hyperelastic material) at large elastic strains.

The algorithms for solving thermoelastoplastic problems at large strains and contact elastic problems at small strains are considered individually and in combination for solving contact thermoelastoplastic problems at large strains. An algorithm for solving thermoelastoplastic problems at large strains is based on the modified method of initial stresses allowing the use of both the constant and the variable tangent stiffness matrices. An algorithm allowing for contact conditions involves the simultaneous consideration of an arbitrary number of deformable bodies in contact. The pairs of nodes with the same coordinates are introduced along the interface. Owing to transformation of the set of FEM equations, the contact conditions reduce to the usual boundary conditions in terms of stresses or displacement with iterative redetermination of their types (adhesion, slip, no contact) in each pair of nodes. Optimum variants of combinations of the iterative procedures allowing for plastic flow and contact interaction are studied.

An attractive feature of the present approach is the simplicity of allowing for the contact conditions for an arbitrary number of deformable bodies in contact and insignificant modifications of computer program which are necessary for the change from small strains to large ones. It should be noted that the present work gives a rigorous derivation of the used constitutive relations and the structure of a tangent stiffness matrix and load vector at arbitrary thermomecanical loading.

A numerical procedure developed for solving contact thermoelastoplastic problems at large strains is realized for an axisymmetric case as software. Testing problems as well as problems on stress–strain state of elements of high pressure apparatus for synthesis of superhard materials have been solved.

2. Constitutive equation

Let us consider a complete system of equations for solving three-dimensional contact thermoelastoplastic problems at large strains. A model of material mechanical behavior at large strains [1, 2] is used. Effect of viscosity and creep are neglected. We assume that at normal pressures the elastic strains are small, at high pressures the shear elastic strains are small and the volumetric elastic strains are finite.

Kinematics

The total deformation gradient tensor is presented as the product

$$\boldsymbol{F} = \frac{\partial \boldsymbol{x}}{\partial \boldsymbol{X}} = \boldsymbol{F}_{e\theta} \cdot \boldsymbol{U}_{p} = \boldsymbol{F}_{e} \cdot \boldsymbol{U}_{\theta} \cdot \boldsymbol{U}_{p} = \boldsymbol{V}_{e} \cdot \boldsymbol{R}_{e} \cdot \boldsymbol{U}_{\theta} \cdot \boldsymbol{U}_{p}\,, \tag{1}$$

where x and X are the position vectors of a point in the deformed and undeformed configurations, respectively; $F_{e\theta}$ and F_e are the thermoelastic and elastic deformation gradient tensors; V_e is the elastic left stretch tensor; U_θ, U_p are the thermal and plastic right stretch tensors, respectively; R_e is the rotation tensor. The tensor U_θ for the isotropic law of thermal expansion is given by $U_\theta = (1 + \alpha\theta)I$, where α is the thermal expansion coefficient; θ is the temperature, I is the unit tensor. However, when solving elastoplastic problems, not the relationships (1) are used but their rate form derived by differentiating (1) with respect to time [1, 2] (see Appendix A)

$$d = \frac{1}{2}\left[\frac{\partial v}{\partial x} + \left(\frac{\partial v}{\partial x}\right)^{\mathrm{t}}\right] = \left(\frac{\partial v}{\partial x}\right)_{\mathrm{s}} = \frac{\overset{\nabla}{B}_e}{a^2} + d_\theta + d_p , \tag{2}$$

$$W = \frac{1}{2}\left[\frac{\partial v}{\partial x} - \left(\frac{\partial v}{\partial x}\right)^{\mathrm{t}}\right] = \left(\frac{\partial v}{\partial x}\right)_{\mathrm{a}} , \qquad d_\theta = \frac{\dot{\overline{(\alpha\theta)}}}{1 + \alpha\theta} I , \qquad a^2 = 1 + \frac{2}{3} I_1(B_e) , \tag{3}$$

where $v = \dot{x}$ is the velocity vector; d, d_θ, d_p are the rates of the total, thermal and plastic deformations, respectively; $\dot{\overline{\alpha\theta}} = \dot{\alpha}\theta + \alpha\dot{\theta}$; $B_e = \frac{1}{2}(V_e \cdot V_e - I)$ is the elastic deformation tensor (which in the numerical algorithm is calculated by integrating Eq. (2) or by inversing the elastic law using known stresses); $I_1(B_e)$ is the first invariant of the B_e; W is the spin tensor characterizing particle rotation rate with respect to the current configuration; $\overset{\nabla}{C} = \dot{C} + 2(C \cdot W)_s$ is the objective Jaumann derivative of the C tensor; $(C)_s$, $(C)_a$ are the symmetric and antisymmetric tensor parts, respectively; a point above indicates the time derivative.

Note that at normal pressure ($I_1(B_e) \ll 1$) and small thermal deformations ($\alpha\theta \ll 1$) it follows that $a^2 \approx 1$, $d_\theta \approx \dot{\overline{(\alpha\theta)}} I$ and the expression (2) can be written in the form

$$d = \overset{\nabla}{B}_e + d_\theta + d_p . \tag{4}$$

The difference between Eq. (4) and the case of small strains lies in the fact that $\overset{\nabla}{B}_e$ is instead of $\dot{B}_e$, and the plastic deformation rate d_p is not a time derivative of the plastic deformation tensor.

Physical relations

In order to separate elastic and plastic modes of deformation, a loading function φ is introduced: at normal pressures

$$\varphi(T, q, \theta) = \sigma_i - \Phi(q, \theta) , \tag{5}$$

at high pressures

$$\varphi(T, q, \theta) = \sigma_i - \Phi(q, \theta)(1 + \kappa\sigma_0) , \tag{6}$$

where T is the Cauchy stress tensor; $q = \int (\frac{2}{3} d_p : d_p)^{1/2}$ is the accumulated plastic strain; $\sigma_0 = \frac{1}{3} I_1(T)$ is the pressure; $\sigma_i = (\frac{3}{2} S : S)^{1/2}$ is the stress intensity; $S = \operatorname{dev} T$ is the deviatoric Cauchy stress tensor; $\Phi(q, \theta)$ is the function to be found experimentally; κ is the material constant (it is assumed that $1 + \kappa\sigma_0 \approx 1$ at normal pressure).

In an elastic region

$$\varphi < 0 \quad \text{or } \varphi = 0 , \qquad \frac{\partial\varphi}{\partial T} : \overset{\nabla}{T} + \frac{\partial\varphi}{\partial\theta}\dot{\theta} < 0 \tag{7}$$

and the physical relations are assumed to be in the form of Hooke law:

at normal pressures

$$T = E(\theta) : B_e = \lambda(\theta) I_1(B_e) I + 2\mu(\theta) B_e , \tag{8}$$

at high pressures

$$T = E(I_1, \theta) : B_e = \lambda(I_1, \theta) I_1(B_e) I = 2\mu(I_1, \theta) B_e , \tag{9}$$

where E is the elastic modulus tensor; λ, μ are the Lame coefficients which depend on θ as well as on

$I_1(\boldsymbol{B}_e)$ at high pressure (the likely ways for concretizing of Eq. (9) are given in Appendix B). For the elastic deformation, in view of Eq. (2) the relationships (8) and (9) in terms of rates take the forms (see Appendix C):

at normal pressures

$$\overset{\nabla}{\boldsymbol{T}} = \boldsymbol{E} : (\boldsymbol{d} - \boldsymbol{d}_\theta) + \frac{\partial \boldsymbol{E}}{\partial \theta} : \boldsymbol{B}_e \dot{\theta} \,, \tag{10}$$

at high pressures

$$\overset{\nabla}{\boldsymbol{T}} = a^2 \boldsymbol{E} : (\boldsymbol{d} - \boldsymbol{d}_\theta) + \dot{\boldsymbol{E}} : \boldsymbol{B}_e \,, \tag{11}$$

where

$$\dot{\boldsymbol{E}} = \frac{\partial \boldsymbol{E}}{\partial I_1(\boldsymbol{B}_e)} I_1(\dot{\boldsymbol{B}}_e) + \frac{\partial \boldsymbol{E}}{\partial \theta} \dot{\theta} = a^2 \frac{\partial \boldsymbol{E}}{\partial I_1(\boldsymbol{B}_e)} [\boldsymbol{I} : (\boldsymbol{d} - \boldsymbol{d}_\theta)] + \frac{\partial \boldsymbol{E}}{\partial \theta} \dot{\theta} \,. \tag{12}$$

In an elastoplastic region

$$\varphi = 0 \,, \quad \frac{\partial \varphi}{\partial \boldsymbol{T}} : \overset{\nabla}{\boldsymbol{T}} + \frac{\partial \varphi}{\partial \theta} \dot{\theta} > 0 \tag{13}$$

and the plastic flow rule is accepted as

$$\boldsymbol{d}_p = \lambda_1 \boldsymbol{S} \,, \quad \lambda_1 \geqslant 0 \,. \tag{14}$$

At normal pressures the plastic flow rule (14) is associated with the yield surface (5), at high pressures Eq. (14) is not associated with the yield surface (6). The condition of plastic incompressibility which follows from Eq. (14), is generally adopted for metals at normal pressures but is taken as an assumption for high pressures (this can be attributed to the fact that at high pressures the intrinsic pores as well as those induced by plastic deformation are closed and the material becomes plastically incompressible).

Computational algorithms do not usually involve Eq. (14) as such, but the quasi-linear relationships between the stress rate and the rates of deformation and temperature which follow from Eqs. (4) and (8) at normal pressures or Eqs. (2) and (9) at high pressures, Eq. (14) and the condition $\dot{\varphi} = 0$ and may be written as (see Appendix C):

at normal pressures

$$\begin{gathered} \overset{\nabla}{\boldsymbol{T}} = \left(\boldsymbol{E} - \frac{1}{\nu} \boldsymbol{E} : \boldsymbol{S} \frac{\partial \varphi}{\partial \boldsymbol{T}} : \boldsymbol{E} \right) : (\boldsymbol{d} - \boldsymbol{d}_\theta) + \frac{\partial \boldsymbol{E}}{\partial \theta} : \boldsymbol{B}_e \dot{\theta} - \frac{1}{\nu} \left(\frac{\partial \varphi}{\partial \boldsymbol{T}} : \frac{\partial \boldsymbol{E}}{\partial \theta} : \boldsymbol{B}_e \dot{\theta} + \frac{\partial \varphi}{\partial \theta} \dot{\theta} \right) \boldsymbol{E} : \boldsymbol{S} \,, \\ \nu = \frac{\partial \varphi}{\partial \boldsymbol{T}} : \boldsymbol{E} : \boldsymbol{S} - \frac{\partial \varphi}{\partial q} \left(\frac{2}{3} \boldsymbol{S} : \boldsymbol{S} \right)^{1/2} , \end{gathered} \tag{15}$$

at high pressures

$$\begin{gathered} \overset{\nabla}{\boldsymbol{T}} = \left(\boldsymbol{E} - \frac{a^2}{\nu} \boldsymbol{E} : \boldsymbol{S} \frac{\partial \varphi}{\partial \boldsymbol{T}} : \boldsymbol{E} \right) : (\boldsymbol{d} - \boldsymbol{d}_\theta) + \dot{\boldsymbol{E}} : \boldsymbol{B}_e - \frac{1}{\nu} \left(a^2 \frac{\partial \varphi}{\partial \boldsymbol{T}} : \dot{\boldsymbol{E}} : \boldsymbol{B}_e + \frac{\partial \varphi}{\partial \theta} \dot{\theta} \right) \boldsymbol{E} : \boldsymbol{S} \,, \\ \nu = a^2 \frac{\partial \varphi}{\partial \boldsymbol{T}} : \boldsymbol{E} : \boldsymbol{S} - \frac{\partial \varphi}{\partial q} \left(\frac{2}{3} \boldsymbol{S} : \boldsymbol{S} \right)^{1/2} , \end{gathered} \tag{16}$$

where $\dot{\boldsymbol{E}}$ is calculated from Eq. (12) both for the elastic and the elastoplastic regions (because in view of Eq. (14) $\boldsymbol{I} : \boldsymbol{d}_p = 0$).

It should be noted that tensor $\overset{\nabla}{\boldsymbol{T}}$ which appears in Eqs. (7) and (13) can be replaced with tensor $\dot{\boldsymbol{T}}$, since for the accepted expressions (5) and (6) for φ the relation $\partial \varphi / \partial \boldsymbol{T} : \overset{\nabla}{\boldsymbol{T}} = \partial \varphi / \partial \boldsymbol{T} : \dot{\boldsymbol{T}}$ is valid (see Appendix C). However, for calculations (when Eqs. (10), (11), (15) and (16) are used), it is convenient to express Eqs. (7) and (13) in terms of $\overset{\nabla}{\boldsymbol{T}}$.

Standard equilibrium equations

$$\frac{\partial}{\partial \boldsymbol{x}} \cdot \boldsymbol{T} + \rho \boldsymbol{f} = 0 \,, \tag{17}$$

where ρ is the mass density and $\boldsymbol{f}$ represents the body forces.

Contact conditions

Now we write friction conditions at the contact boundary S_c for the case of large strains in the three-dimensional case, and write them in scalar form for deformed state in the local coordinate system formed by singular normal $\boldsymbol{r}_n$ and vectors $\boldsymbol{r}_i$, $\boldsymbol{r}_j$ tangential to the contact surface of the first body.

$$\left.\begin{array}{l} T_n^1 = -T_n^2 \leqslant 0 \,; \qquad T_m^1 = -T_m^2 \,, \quad m = i, j \qquad (18) \\ u_n^1 - u_n^2 \leqslant \delta \begin{cases} u_n^1 - u_n^2 < \delta \,, & \Rightarrow T_n^1 = T_i^1 = T_j^1 = 0 \qquad (19) \\ u_n^1 - u_n^2 = \delta \,, & \Rightarrow T_n^1 \leqslant 0 \qquad (20) \end{cases} \end{array}\right\} S_c$$

$$\left.\begin{array}{l} F^*(T_n^1, T_i^1, T_j^1) \leqslant 0 \\ m = i, j \end{array} \begin{cases} F^*(T_n^1, T_i^1, T_j^1) < 0 \,, & \Rightarrow \dot{u}_m^2 - \dot{u}_m^1 = 0 \,, \qquad (21) \\ F^*(T_n^1, T_i^1, T_j^1) = 0 \,, & \Rightarrow \dot{u}_m^2 - \dot{u}_m^1 = \lambda_2 \dfrac{\partial F^*(T_n^1, T_i^1, T_j^1)}{\partial T_m^1} \,, \qquad (22) \end{cases}\right\} S_c^1 \cup S_c^2$$

where T_n, T_i, T_j are the normal stress and the stresses tangential to the contact surface, $T_n = \boldsymbol{r}_n \cdot \boldsymbol{T} \cdot \boldsymbol{r}_n$; $T_m = \boldsymbol{r}_m \cdot \boldsymbol{T} \cdot \boldsymbol{r}_n$, $m = i, j$; indexes 1 and 2 identify those belonging to the first and the second bodies, respectively; u_n, $\dot{u}_n$, u_m, $\dot{u}_m$, $m = i, j$ are, respectively, the components of displacement and velocity vectors in the local coordinate system, δ is the gap; $F^*(T_n, T_i, T_j) = 0$ is the friction surface; $\lambda_2 \geqslant 0$ is the scalar parameter. Thus, for the isotropic Coulomb law of friction, the surface $F^*(T_n, T_i, T_j)$ is written as

$$F^*(T_n\, T_i, T_j) = \frac{1}{\gamma} [(T_i)^2 + (T_j)^2]^{1/2} + T_n \,, \tag{23}$$

where γ is the friction coefficient. Then, the slipping law (22) reduces to

$$\dot{u}_m^2 - \dot{u}_m^1 = \lambda_2 T_m^1 \,, \qquad \lambda_2 \geqslant 0 \,, \quad m = i, j \,. \tag{24}$$

In the axisymmetric case, circumferential tangential stress and displacement are equal to zero, and normal $\boldsymbol{r}_n$ and tangential $\boldsymbol{r}_j$ to the first body surface singular vectors are arranged in an axial section, Eqs. (23) and (24) taking the form

$$F^*(T_n, T_j) = \frac{1}{\gamma} |T_j| + T_n \,, \tag{25}$$

$$\dot{u}_j^2 - \dot{u}_j^1 = \lambda_2 T_j^1 \,, \quad \lambda_2 \geqslant 0 \,. \tag{26}$$

The relationships (2)–(22), when supplemented with boundary conditions, constitute a comprehensive system of equations for solving contact thermoelastoplastic problems.

3. Numerical technique

For the FEM solution of the above system of differential equations the equilibrium equations (17) may be written in variational form following the principle of virtual work (weak form)

$$\int_V \boldsymbol{T} : \boldsymbol{d}^* \, \mathrm{d}V = \int_S \boldsymbol{t} \cdot \boldsymbol{u}^* \, \mathrm{d}S + \int_V \rho \boldsymbol{f} \cdot \boldsymbol{u}^* \, \mathrm{d}V \,, \tag{27}$$

where $\boldsymbol{u}^*$ are virtual displacements, $\boldsymbol{d}^* = (\partial \boldsymbol{u}^* / \partial \boldsymbol{x})_s$; $\boldsymbol{t}$, $\boldsymbol{f}$ are the surface tractions (including contact forces) and body forces, respectively; V, S are the volume and surface of the body in the current configuration.

Consider the FE form of Eq. (27). Using indicial notation, the rectangular Cartesian coordinate system and introducing the standard approximation

$$u_i^* = \Psi_{i\alpha}(x_m)\bar{u}_\alpha^* , \qquad d_{ij}^* = \frac{1}{2}\left(\frac{\partial \Psi_{i\alpha}}{\partial x_j} + \frac{\partial \Psi_{j\alpha}}{\partial x_i}\right)\bar{u}_\alpha^* , \tag{28}$$

or

$$\{u^*\} = [N]\{\bar{u}^*\} , \qquad \{d^*\} = [B]\{\bar{u}^*\} , \tag{29}$$

(where $\Psi_{i\alpha}(x_m)$ are the known interpolation functions, $\bar{u}_\alpha^*$ are the nodal values of components of the vertual displacements vector; $i, j, m = 1, 2, 3$; $\alpha = 1, 2, \ldots, 3 \times M$, M is the number of nodes; Eq. (29) is the standard FE notation of Eq. (28) in matrix form) we have

$$\int_V \underbrace{\frac{1}{2}\left(\frac{\partial \Psi_{i\alpha}}{\partial x_j} + \frac{\partial \Psi_{j\alpha}}{\partial x_i}\right)}_{[B]^t} T_{ij}\, \mathrm{d}V = \int_S t_i \Psi_{i\alpha}\, \mathrm{d}S + \int_V \rho f_i \Psi_{i\alpha}\, \mathrm{d}S \tag{30}$$

or

$$\int_V [B]^t\{T\}\, \mathrm{d}V = \{q\} , \qquad \{q\} = \int_S [N]^t\{t\}\, \mathrm{d}S + \int_V [N]^t\{\rho f\}\, \mathrm{d}V . \tag{31}$$

It should be noted that Eqs. (27)–(31), written in the current configuration, are of the same form for both small and large strains.

The use of FEM involves FE approximation of displacements, strains and stresses and the solution of a continuous problem reduces to the determination of the parameters under study in a finite number of nodes of the FE mesh so that the solution obtained should satisfy Eqs. (2)–(16), (31) and contact and boundary conditions.

To solve the above set of equations, a numerical technique has been developed which consists of three parts: (a) a procedure for solving thermoelastoplastic problems at large strains; (b) a procedure for solving contact elastic problems at small strains [31]; (c) a combined procedure for solving contact thermoelastoplastic problems at large strains.

The solution of the class of problems under discussion depends on history of deformation, therefore it is realized in step-by-step form, i.e. with a known solution at the instant of time t_{N-1} one should find a solution at the instant of time $t_N = t_{N-1} + \Delta t$, where N is the step number. It should be also noted that the numerical techniques developed do not formally distinguish between normal and high pressures (at normal pressures some simpler relations given above are used).

3.1. *The procedure for solving thermoelastoplastic problems at large strains*

The procedure for solving thermoelastoplastic problems at large strains is based on the stepwise solution using the method of initial stresses. The solution is made using a variable reference configuration which coincides with the deformed configuration at the previous solution step. The algorithm used can be easily given by

$$\begin{array}{ll}
(1) & \{\Delta\bar{u}\} = 0 ; \quad \{\Psi_0\} = \{\Delta q_0\} ; \quad i = 0 ; \\
(2) & i = i + 1 ; \quad \{\Delta\bar{u}_i\} = \bar{\gamma}[K]^{-1}\{\Psi_{i-1}\} ; \\
(3) & \{\Delta\bar{u}\} = \{\Delta\bar{u}\} + \{\Delta\bar{u}_i\} ; \quad \{\Delta T\} = \{\Delta T(\{\Delta\bar{u}\}, \Delta\theta)\} ; \quad \{x_i\} = \{x\} + \{\Delta\bar{u}\} ; \\
 & \{\Psi_i\} = \{q_i\} - \int_{V+\Delta V} [B]^t(\{T\} + \{\Delta T\})\, \mathrm{d}V ; \\
(4) & \text{Is the convergence achieved } (\|\Psi_i\| < \varepsilon)? \\
 & \text{no} \rightarrow (2) \qquad \downarrow \text{yes} \rightarrow (5) \\
(5) & N = N + 1 ; \quad \{x\} = \{x\} + \{\Delta\bar{u}\} ; \quad \{T\} = \{T\} + \{\Delta T\}
\end{array} \tag{32}$$

Here, N is the step number, i is the iteration number, $\{x\}$, $\{x_i\}$ are the vectors of nodal coordinates at the beginning of a step and after the ith iteration of the Nth step, respectively; $\{\bar{u}\}$ is the nodal displacement vector; $[K]$ is the stiffness matrix (either constant elastic or variable tangent stiffness matrix (see Appendix D) may be used, as the problem solution depends only indirectly on the type of the $[K]$ matrix defining the convergence rate of an iterative process); $\{\Psi_i\}$ is the residual of the FE equilibrium equation (31) written for the i-th iteration in the current configuration;

$$\{q_i\} = \int_{S+\Delta S} [N(\{x_i\})]^{\mathrm{t}}(\{t\} + \{\Delta t\})\,\mathrm{d}S + \int_{V+\Delta V} [N(\{x_i\})]^{\mathrm{t}}(\{\rho f\} + \{\Delta(\rho f)\})\,\mathrm{d}V$$

is the load vector in ith iteration of the Nth step of loading;

$$\{\Delta q_0\} = \int_S [N(\{x\})]^{\mathrm{t}}\{\Delta t\}\,\mathrm{d}S + \int_V [N(\{x\})]^{\mathrm{t}}\{\Delta(\rho f)\}\,\mathrm{d}V$$

is the initial value of the incremental load vector at the Nth step; $[N(\{x_i\})]$, $[B(\{x_i\})]$ are the standard FE matrices (see Eq. (29)) written in current configuration $\{x_i\}$ of the Nth step); $\|\Psi_i\| = (\{\Psi_i\}^{\mathrm{t}}\{\Psi_i\})/(\{q_i\}^{\mathrm{t}}\{q_i\})$ is the residual vector norm; ε is the preset accuracy; $\{T\}$ is the stress vector at the beginning of the Nth step; Δ denotes increment of a quantity; $\bar{\gamma}$ is the scalar parameter which permits accelerating the convergence of iteration process (may be determined by a numerical experiment and may be varied with the number of iteration; in the simplest variant $\bar{\gamma} = 1$).

Let us discuss the algorithms. It should be noted once more that all the components of stress and strain tensors are written in common Cartesian coordinates (or in cylindrical coordinates if the problem is axisymmetric) for any deformed configuration both at the beginning and at the end of the step of loading. This means that the components' form of the representation of Eqs. (2)–(16) is derived from the tensor one by replacing the tensor notations in Eqs. (2)–(16) with their components in Cartesian coordinate system. Only the Cauchy stress tensor is used in the proposed algorithm.

The sequence of the calculation at loading step N is the following:

(a) The $\{\Delta\bar{u}_i\}$ increment of displacement at the ith iteration of loading step N is calculated by solving the $\{\Delta\bar{u}_i\} = \bar{\gamma}[K]^{-1}\{\Psi_{i-1}\}$ system.

(b) Then, $\{\Delta\bar{u}\} = \{\Delta\bar{u}\} + \{\Delta\bar{u}_i\}$, i.e. overall displacement increment for ith iterations at loading step N is determined. Using relations (10), (15) or (11), (16) and known $\{\Delta\bar{u}\}$ and $\Delta\theta$, increment of stress $\{\Delta T\} = \{\Delta T(\{\Delta\bar{u}\}, \Delta\theta)\}$ is calculated (in more detail below).

It should be noted that from algorithm (32), the displacement increment $\{\Delta\bar{u}\}$ as well as the stress increment $\{\Delta T\}$ are calculated for each iteration of the Nth loading step, beginning from the end of the preceding step (which is of a deformed configuration obtained at the $N-1$th step). This permits the unstable calculations to be eliminated in determining stresses when at various iterations of the Nth step of loading at the same point the repeated alternation of plastic loading and elastic unloading can take place.

(c) Then we calculate the residual of equilibrium equations written in a current configuration at the ith iteration

$$\{\Psi_i\} = \{q_i\} - \int_{V+\Delta V} [B(\{x_i\})]^{\mathrm{t}}(\{T\} + \{\Delta T\})\,\mathrm{d}V\,. \tag{33}$$

If the convergence is not reached, i.e. $\|\Psi_i\|$ exceeds some preset number ε, we return to point (a).

(d) We calculate new coordinates $\{x\} = \{x\} + \{\Delta\bar{u}\}$ and stresses $\{T\} = \{T\} + \{\Delta T\}$ at the end of the Nth loading step which serve as the initial data for $N+1$th step of loading.

Let us consider the item (b) in greater detail. In works [3, 23] in order to determine stresses from known displacements at elastoplastic straining one uses an approximate 'return mapping algorithm' in which the plastic strain increment direction is given according to the plastic flow rule for stress values at the end of the loading step. In this case within the step, this direction remains without changes even at large displacement and strain increments, and a scalar value of plastic strain increment is found, in the general case, through the solution of a non-linear scalar equation by the iterative method.

The present work uses a precise numerical integration of constitutive equations. Now we consider peculiarities of this procedure. The sequence of $\mathrm{d}\boldsymbol{T} = \dot{\boldsymbol{T}}\,\mathrm{d}t$, $\mathrm{d}\boldsymbol{B}_{\mathrm{e}} = \dot{\boldsymbol{B}}_{\mathrm{e}}\,\mathrm{d}t$ and $\mathrm{d}q = \dot{q}\,\mathrm{d}t$ calculations in terms of known values of displacement increment $\mathrm{d}\boldsymbol{u} = \boldsymbol{v}\,\mathrm{d}t$ and temperature increment $\mathrm{d}\theta = \dot{\theta}\,\mathrm{d}t$ for the case of high pressures is as follows (at normal pressure the procedure is similar). First, we determine $\boldsymbol{d}$ from Eq. (2) and $\boldsymbol{W}$ and $\boldsymbol{d}_\theta$ from Eq. (3). Then, assuming the strains to be elastic, we find $\overset{\nabla}{\boldsymbol{T}}$ (from Eq. (11)), $\dot{\boldsymbol{T}} = \overset{\nabla}{\boldsymbol{T}} - 2(\boldsymbol{T}\cdot\boldsymbol{W})_{\mathrm{s}}$ and $\mathrm{d}\boldsymbol{T} = \dot{\boldsymbol{T}}\,\mathrm{d}t$. Then we check the condition $\varphi(\boldsymbol{T} + \mathrm{d}\boldsymbol{T}, q, \theta + \Delta\theta) \leq 0$ (this is equivalent to condition (7)). If it is valid we suggest that $\mathrm{d}\boldsymbol{T}$ has been correctly calculated. Otherwise, we take strains to be elastoplastic and $\overset{\nabla}{\boldsymbol{T}}$ is found from Eq. (16). In case of elastoplastic straining we determine $\boldsymbol{d}_{\mathrm{p}}$ and $\mathrm{d}q = \dot{q}\,\mathrm{d}t = (\frac{2}{3}\boldsymbol{d}_{\mathrm{p}} : \boldsymbol{d}_{\mathrm{p}})^{1/2}\,\mathrm{d}t$ from the relation (C.9) (see Appendix C) and Eq. (14). It follows from Eq. (2) that

$$\dot{\boldsymbol{B}}_{\mathrm{e}} = \left[1 + \frac{2}{3} I_1(\boldsymbol{B}_{\mathrm{e}})\right](\boldsymbol{d} - \boldsymbol{d}_\theta - \boldsymbol{d}_{\mathrm{p}}) - 2(\boldsymbol{B}_{\mathrm{e}}\cdot\boldsymbol{W})_{\mathrm{s}}\,. \tag{34}$$

Alternatively, $\dot{\boldsymbol{B}}_{\mathrm{e}}$ can be also calculated from known $\overset{\nabla}{\boldsymbol{T}}$ and $\boldsymbol{T}$ by inversing the thermoelastic law (9), whenever possible, and differentiating it. Thus, to solve the thermoelastoplastic problem, it is sufficient to calculate $\boldsymbol{T}$, $\boldsymbol{B}_{\mathrm{e}}$, q and the total displacement $\boldsymbol{u}$ (the calculation of $\boldsymbol{U}_{\mathrm{e}}$, $\boldsymbol{U}_\theta$, $\boldsymbol{U}_{\mathrm{p}}$, $\boldsymbol{R}_{\mathrm{e}}$ are not needed here).

We describe now the sequence of calculations of $\{\Delta T\}$ in case of large values of $\{\Delta\bar{u}\}$ and $\Delta\theta$ for algorithm (32). First, we assume stress increment to be elastic, and to determine $\{\Delta T\}$ we use relation (11) (in the same way as in determining $\mathrm{d}\boldsymbol{T}$) Then, we check the condition

$$\varphi_2 = \varphi(\{T\} + \{\Delta T\}, q, \theta + \Delta\theta) \leq 0\,.$$

If it is valid, then stresses $\{\Delta T\}$ have been correctly calculated. At $\varphi_2 > 0$, one has to determine the moment of transition of straining from the elastic region into the elastoplastic one (when $\varphi_1 = \varphi(\{T\}, q, \theta) = 0$, this need not be done). The moment of the straining transition from the elastic region into elastoplastic one is determined by the following procedure [32]. Let, at the beginning of the step, $\varphi_1 = \varphi(\{T\}, q, \theta) < 0$. Using the algorithm (32) and known $\{\Delta\bar{u}\}$, $\Delta\theta$ we find stresses $\{\Delta T\}$ with the use of the elastic law (11) (in the same way as in determining $\mathrm{d}\boldsymbol{T}$). Let, in this case, $\varphi_2 = \varphi(\{T\} + \{\Delta T\}, q, \theta + \Delta\theta) > 0$. Then, $\tau = 0 \div 1$ parameter has to be determined, which will characterize the attainment to the yield surface, i.e.

$$\varphi_3 = \varphi(\{T\} + \{\Delta T(\tau\{\Delta\bar{u}\}, \tau\,\Delta\theta)\}, q, \theta + \tau\,\Delta\theta) = 0\,. \tag{35}$$

Expanding φ function into Tailor series and restricting ourselves to derivatives of the first order we obtain

$$\tau = -\frac{\varphi_1}{\varphi_2 - \varphi_1}\,. \tag{36}$$

If, after the calculation of τ from Eq. (36), $|\varphi_3| > \varepsilon_1$ here ε_1 is a given tolerance), then τ value can be refined similarly by iteration, using parameters φ_3 and φ_1 (or φ_2) as initial and final values of φ function.

Thus, when straining by $\tau\{\Delta\bar{u}\}$, $\tau\,\Delta\theta$ in calculating $\{\Delta T\}$ one has to apply relation (11). In further straining by $(1-\tau)\{\Delta\bar{u}\}$, $(1-\tau)\,\Delta\theta$, the interval $(1-\tau)\{\Delta\bar{u}\}$, $(1-\tau)\,\Delta\theta$ must be divided into small values, and $\{\Delta T\}$ value is to be defined by numerical integration (using the relation (16)). The number of divisions of the integration interval can be determined numerically from the condition that relation $\varphi(\{T\} + \{\Delta T\}, q + \Delta q, \theta + \Delta\theta) \approx 0$ is satisfied. Note that in elastic region (interval $\tau\,\Delta\bar{u}$, $\tau\,\Delta\theta$) stress increment $\{\Delta T\}$ was calculated from Eq. (11) using finite values of $\tau\{\Delta\bar{u}\}$, $\tau\,\Delta\theta$. However, in the case of large values of $\tau\{\Delta\bar{u}\}$, $\tau\,\Delta\theta$, in order to calculate $\{\Delta T\}$ increment, one can also divide interval $\tau\,\Delta\bar{u}$, $\tau\,\Delta\theta$ into smaller values and to perform numerical integration. A numerical experiment has demonstrated that the time for integrating constitutive relations by using the above procedure is much less than the time for FEM solving the linear system of equations.

In case of small rotations $\boldsymbol{W} \approx 0$ and at normal pressure $(I_1(\boldsymbol{B}_{\mathrm{e}}) \ll 1)$, the given algorithm (32) for solving thermoelastoplastic problems at large plastic strains completely coincides in form with that for the case of small strains, only $\{x\} = \{x\} + \{\Delta \bar{u}\}$ coordinates should be redetermined at large strains.

Let us compare the present approach based on the initial stress method at large strains with known ones. All of them are based on the calculation of tangent stiffness matrix which may have different forms depending on a formulation used (Lagrangian or updated Lagrangian formulation) and chosen measures of stresses, strains and constitutive equations. The tangent stiffness matrix is calculated using a rate form of the principle of virtual work. This may cause violation of the equilibrium equations for finite values of stresses. When using the present approach, the equilibrium equations (31) are satisfied for the finite values of stresses ($\|\Psi_i\| < \varepsilon$, see Eq. (32)) to a preset accuracy. The algorithm (32) permits the use of both constant elastic and variable tangent stiffness matrices. This is due to the fact that the stiffness matrix has no explicit effect on the fulfilment of equilibrium equations but it governs the rate of convergence of iteration process (though 'wrong' choice of a stiffness matrix may lead to weak convergence or divergence). An attractive feature of the present approach is the simplicity of transition from the case of small strains to that of large strains owing to proper choice of measures of stresses and strains and to iteration scheme of the problem solution.

3.2. *A procedure for solving contact elastic problems at small strains*

Let us represent the algorithm of solving contact elastic problems at small strains in case of FEM discretization for an arbitrary geometry of the contact surface, rather common laws of contact friction, an arbitrary number of interacted deformable bodies (preserving symmetrical stiffness matrix of the linear algebraic equation system). It is based on combined consideration of bodies in contact. The pairs of nodes with the same coordinates are introduced along the contact boundary (Fig. 1). Because of the presence of energy dissipation in friction, the problem must be solved step-by-step in terms of increments.

The friction conditions (18)–(22) in view of FE discretization may be written as follows.

Let nodes A and B be in contact and belong to bodies 1 and 2, respectively. Then

$$\bar{t}_p^A + \bar{t}_p^B = 0\,, \qquad \bar{t}_n^A \leq 0\,, \quad p = n, i, j \tag{37}$$

if

$$F(\bar{t}_n^A, \bar{t}_i^A, \bar{t}_j^A) < 0\,, \quad \text{then} \quad \Delta\bar{u}_p^A - \Delta\bar{u}_p^B = 0\,, \quad (p = n, i, j)\,, \tag{38}$$

if

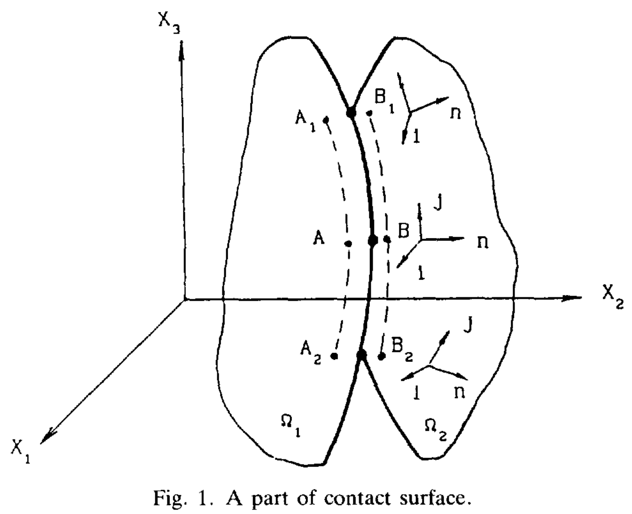

Fig. 1. A part of contact surface.

$$F(\bar{t}_n^A, \bar{t}_i^A, \bar{t}_j^A) = 0\,, \quad \text{then} \quad \Delta\bar{u}_n^A - \Delta\bar{u}_n^B = 0\,, \qquad \Delta\bar{u}_m^A - \Delta\bar{u}_m^B = \Delta\bar{u}_m^{AB} = \lambda_2 \frac{\partial F(\bar{t}_n^A, \bar{t}_i^A, \bar{t}_j^A)}{\partial \bar{t}_m^A}\,,$$
$$\lambda_2 \geq 0\,, \quad m = i, j\,. \tag{39}$$

Assume that there is no contact between the points A and B. Then

$$\bar{t}_p^A = \bar{t}_p^B = 0\,, \qquad \bar{u}_n^A - \bar{u}_n^B < \delta\,, \quad p = n, i, j\,. \tag{40}$$

Here, $\bar{t}_p$, $\bar{u}_p$, $p = n$, i, j are the components of load vector due to contact forces and the nodal displacements vector in a local orthogonal coordinate system formed by vectors which are normal and tangential to the surface of the first body ($\boldsymbol{r}_n$ and $\boldsymbol{r}_i$, $\boldsymbol{r}_j$, respectively); the superscripts A and B denote those belonging to the respective nodes, and δ is the gap; Δu_m^{AB} are the components of point B sliding vector with respect to point A; $F(\bar{t}_n^A, \bar{t}_i^A, \bar{t}_j^A)$ is the function of friction (for Coulomb's friction law $F(\bar{t}_n^A, \bar{t}_i^A, \bar{t}_j^A) = 1/\gamma[(\bar{t}_i^A)^2 + (\bar{t}_j^A)^2]^{1/2} + \bar{t}_n^A$, γ is the coefficient of friction). In contact nodes the load vector due to contact forces $\{\bar{t}\}$ is given by

$$\{\bar{t}\} = \int_V [B]^{\mathrm{t}}\{T\}\,\mathrm{d}V - \int_V [N]^{\mathrm{t}}\{\rho f\}\,\mathrm{d}V = \{q\} - \{\bar{f}\}\,, \qquad \{\bar{f}\} = \int_V [N]^{\mathrm{t}}\{\rho f\}\,\mathrm{d}V\,, \tag{41}$$

which follows from Eq. (31). Here, $\{\bar{f}\}$ is the load vector due to body forces.

Let us rearrange the relationship (39). Since one of the tangential vectors $\boldsymbol{r}_i$ or $\boldsymbol{r}_j$ is chosen arbitrarily to an accuracy of a rotation, $\boldsymbol{r}_j$ is specified as being coincident with the direction of possible slipping, i.e. such that $\partial F(\bar{t}_n, \bar{t}_i, \bar{t}_j)/\partial \bar{t}_i^A = 0$. For example, in the case of Coulomb's friction, this means that $\partial F/\partial \bar{t}_i = 1/\gamma\, \bar{t}_i^A = 0$. Then, for a new position of $\boldsymbol{r}_i$ and $\boldsymbol{r}_j$ vectors, the relationship (39) can be rewritten as

$$\text{if} \quad F(\bar{t}_n^A, \bar{t}_i^A\, \bar{t}_j^A) = 0\,, \quad \text{then} \quad \Delta\bar{u}_m^A - \Delta\bar{u}_m^B = 0\,, \qquad \Delta\bar{u}_j^A - \Delta\bar{u}_j^B = \Delta\bar{u}_j^{AB} = \lambda_2 \frac{\partial F(\bar{t}_n^A, \bar{t}_i^A, \bar{t}_j^A)}{\partial \bar{t}_j^A}\,,$$
$$\lambda_2 \geq 0\,, \quad m = n, i\,. \tag{42}$$

Hereafter, we assume that the tangential vector $\boldsymbol{r}_j$ coincides with the direction of possible slip and use Eq. (42) instead of Eq. (39) (in the case of plane and axisymmetric problems, $\boldsymbol{r}_j$ is determined in a unique manner and lies in the plane, for which the calculation is carried out, or in the axial section, respectively).

The FEM solution of the contact elastic problem in terms of increments reduces to the solution of linear algebraic equations at Nth step of loading

$$[K]\{\Delta\bar{u}\} = \{\Delta q\}\,. \tag{43}$$

It should be noted that the conditions $(37)_1$ and $(40)_1$, when represented in terms of increments and with account of Eq. (41), have the respective forms

$$\Delta q_p^A + \Delta q_p^B = \Delta\bar{f}_p^A + \Delta\bar{f}_p^B\,, \quad p = n, i, j\,, \tag{44}$$

$$\Delta q_p^A = \Delta\bar{f}_p^A\,, \quad \Delta q_p^B = \Delta\bar{f}_p^B\,, \quad p = n, i, j\,, \tag{45}$$

where $\Delta\bar{f}_p^A$, $\Delta\bar{f}_p^B$ are the known components of increment of the load vector due to body forces.

For simplicity sake assume that for Eq. (43), load vector due to thermal strains is included into the vector $\{\bar{f}\}$.

REMARK 1. The relationships (37)–(45) and the iterative procedure described below hold true for both small and large strains; for large strains Eqs. (37)–(42) are written for the current deformed configuration ($\{T\}$ and $[B]$ in (41) are the Cauchy stress vector and the standard kinematic matrix calculated for the current configuration, respectively; $[K]$ is tangent elastic stiffness matrix at large strains).

REMARK 2. In discretization of problems by FEM, the account of boundary conditions reduces to their applying in nodes of FE mesh along the boundary. Contact problems are the problems with unknown boundary conditions at the contact surface which are to satisfy friction conditions. The conditions of contact friction (37)–(40) are written for such a case of the arrangement of a pair of interacting contact nodes, when their coordinates coincide or differ slightly by values of small displacements (i.e. the solution of the contact problem reduces to the fulfilment of the conditions of friction in pairs of contact nodes). If when solving the problem, the coordinates of the interacting contact nodes start to differ considerably, then at a definite step of the problem solution one should redetermine the FE mesh. Thus, the contact surface is formed by contact pairs of nodes whose coordinates coincide or their difference may be neglected.

Since the components of vectors $\{\Delta \bar{u}\}$ and $\{\Delta q\}$ in Eq. (43) are written in the global coordinate system and the contact conditions (37)–(40) are formulated in the local coordinate system, the system (43) may be modified as follows

$$[\tilde{K}]\{\Delta \tilde{u}\} = \{\Delta \tilde{q}\}\,, \tag{46}$$

where $[\tilde{K}] = [\beta]^{t}[\alpha]^{t}[K][\alpha][\beta]$ is the symmetric matrix, $\{\Delta \tilde{u}\} = [\beta][\alpha]\{\Delta \bar{u}\}$, $\{\Delta \tilde{q}\} = [\beta][\alpha]\{\Delta q\}$ (the matrices $[\alpha]$ and $[\beta]$ are given in Appendix E). The elements of the $\{\Delta \tilde{u}\}$ and $\{\Delta \tilde{q}\}$ vectors for the nodes beyond the contact surface are equal to those of the $\{\Delta \bar{u}\}$ and $\{\Delta q\}$ vectors; for nodes in the contact surfaces

$$\Delta \tilde{u}_p^{+} = \frac{\sqrt{2}}{2}(\Delta \bar{u}_p^{A} + \Delta \bar{u}_p^{B})\,; \qquad \tilde{u}_p^{-} = \frac{\sqrt{2}}{2}(\Delta \bar{u}_p^{A} - \Delta \bar{u}_p^{B})\,; \tag{47}$$

$$\Delta \tilde{q}_p^{+} = \frac{\sqrt{2}}{2}(\Delta q_p^{A} + \Delta q_p^{B}) = \frac{\sqrt{2}}{2}[(\Delta \bar{t}_p^{A} + \Delta \bar{t}_p^{B}) + (\Delta \bar{f}_p^{A} + \Delta \bar{f}_p^{B})]\,; \tag{48}$$

$$\Delta \tilde{q}_p^{-} = \frac{\sqrt{2}}{2}(\Delta q_p^{A} - \Delta q_p^{B}) = \frac{\sqrt{2}}{2}[(\Delta \bar{t}_p^{A} - \Delta \bar{t}_p^{B}) + (\Delta \bar{f}_p^{A} - \Delta \bar{f}_p^{B})]\,; \quad p = n, i, j\,, \tag{49}$$

where $\Delta \bar{u}_p$, Δq_p, $\Delta \bar{t}_p$, $\Delta \bar{f}_p$ are the incremental components of the nodal displacement vector, load vector, the load vector due to contact and body forces written in the local coordinate system, respectively; the superscripts A and B correspond to points A and B.

Now we present an iterative procedure of solving contact elastic problems. Consider two cases:

(a) The contact surface does not change. In the first iteration, we solve the system (46) with adhesion conditions $(38)_2$, (44) in all pairs of nodes at the contact boundary which is equivalent to conditions $\Delta \tilde{u}_p^{-} = 0$, $\Delta \tilde{q}^{+} = \sqrt{2}/2\,(\Delta \bar{f}_p^{A} + \Delta \bar{f}_p^{B}) = \Delta q_p^{a}$, $p = n, i, j$; Δq_p^{a} is a known value. It should be noted that in case of the given interference ($\Delta \bar{u}_n^{A} - \Delta \bar{u}_n^{B} = \delta$, $\delta < 0$), the kinematic boundary conditions $\Delta \tilde{u}_n^{-} = \delta$ should be imposed on the system (46). On solving the system (46) we check the friction condition $F(\bar{t}_n^{S}, \bar{t}_i^{S}, \bar{t}_j^{S}) \geq 0$, here S is the iteration number (a total increment of displacement at the Sth iteration of the Nth step of loading is equal to the sum of increments of displacements for all the S-number previous iterations of the Nth step). If the friction condition $F(\bar{t}_n^{S}, \bar{t}_i^{S}, \bar{t}_j^{S}) > 0$ is not satisfied at some contact nodes, we determine from Eq. (39) a new direction of the possible slipping and redetermine the position of $\boldsymbol{r}_i$ and $\boldsymbol{r}_j$ vectors to satisfy the condition (42). Then, from the condition $F(\bar{t}_n^{S}, \bar{t}_i^{S}, \bar{t}_j^{S+1}) = 0$ we find $\bar{t}_j^{S+1}$ and $\Delta \bar{t}_j^{S+1} = \bar{t}_j^{S+1} - \bar{t}_j^{S}$ for $S + 1$th iteration. Since the direction of the possible slipping can vary at different iterations, then for $S + 1$th iteration of the Nth step one must project the slipping vector for S-number of previous iterations on the new slipping direction (determined on solving the system (46) at the Sth iteration) and to put $\Delta \tilde{u}_i^{-} = -\Delta \bar{u}_i^{AB}$ (where $\Delta \bar{u}_i^{AB}$ is the projection of the slipping vector for the S-number of previous iterations on $\boldsymbol{r}_i$ new direction). Vectors $\bar{t}_j^{S}$ and $\bar{t}_n^{S}$ are calculated from Eq. (41) by the solving of the problem at the Sth iteration of the Nth step of loading. It should be noted that as $\Delta \bar{f}_p^{A}$ and $\Delta \bar{f}_p^{B}$ ($p = n, i, j$) in Eqs. (48), (49) are practically independent of iteration then with account of Eq. (44) for all iterations beginning from the second one

$$\Delta \tilde{q}_p^{+} = 0\,; \qquad \Delta \tilde{q}_p^{-} = \frac{\sqrt{2}}{2}(\Delta \bar{t}_p^{A} - \Delta \bar{t}_p^{B})\,; \quad p = n, i, j\,. \tag{50}$$

Imposing constraints $\Delta\tilde{u}_p^- = 0$, $\Delta\tilde{q}_p^+ = 0$ ($p = n, i, j$) on the system (46) at those contact nodes where $F(\bar{t}_n^S, \bar{t}_i^S, \bar{t}_j^S) < 0$, and imposing constraints $\Delta\tilde{u}_n^- = 0$, $\Delta\tilde{u}_i^- = -\Delta\bar{u}_i^{AB}$, $\Delta\tilde{q}_p^+ = 0$ and giving the increment of load vector $\Delta\tilde{q}_j^- = \sqrt{2}/2\ (\Delta\bar{t}_j^A - \Delta\bar{t}_j^B) = \Delta q_j^b$ at those contact nodes where $F(\bar{t}_n^S, \bar{t}_i^S, \bar{t}_j^S) \geqslant 0$ ($\Delta\bar{u}_i^{AB}$, Δq_j^b are the known values, $p = n, i\ j$), we obtain a set of equations for finding out the increments of displacements at the $S+1$th iteration of the Nth step of loading. Then, having solved the system (46) at the $S+1$th iteration we check the conditions $F(\bar{t}_n^{S+1}, \bar{t}_i^{S+1}, \bar{t}_j^{S+1}) \leqslant 0$ for new values of load vector $\{\bar{t}\}$. The iteration process ceases when the condition $F(\bar{t}_n, \bar{t}_i, \bar{t}_j) \leqslant 0$ is satisfied at all contact nodes.

(b) The contact surface changes (i.e. the number of pairs of nodes being in contact varies). In this case additional standard check $\bar{t}_n \leqslant 0$ and the conditions of the mutual impenetration $(40)_2$ should be made.

It should be noted that in case of contact problems with a variable contact area, a final contact boundary is known from some considerations, and at contact nodes the conditions of adhesion or zero friction are given, then the problem can be solved without iteration as the problems with a constant contact surface. In this case for corresponding contact nodes a negative gap (i.e. interference) should be given (δ_1) which equals the gap value between them at the initial state.

Summing up the above procedure one may conclude that the solution of the contact thermoelastic problem reduces to the solving of a symmetrical system of equations (46) with constant dimensions NN (NN = triple or twice the number of nodes for three-dimensional or plane cases, respectively), types of contact conditions being as follows:

Adhesion conditions

$$\Delta\tilde{u}_p^- = 0 \quad (\text{or } \Delta\tilde{u}_n^- = \delta_1)\,; \qquad \Delta\tilde{q}_p^+ = \Delta q_p^a\,; \quad p = n, i, j\,.$$

Slipping conditions

$$\Delta\tilde{u}_n^- = \delta\,; \qquad \Delta\tilde{u}_i^- = \delta_2\,; \qquad \Delta\tilde{q}_j^- = q_j^b\,; \qquad \Delta\tilde{q}_p^+ = \Delta q_p^a\,; \quad p = n, i, j\,.$$

No-contact conditions

$$\Delta\tilde{q}_p^- = \Delta q_p^c\,; \qquad \Delta\tilde{q}_p^+ = \Delta q_p^d\,; \quad p = n, i, j\,.$$

There, δ_1, δ_2, Δq_p^a, Δq_j^b, Δq_p^c, Δq_p^d, $p = n, i, j$ are the known values, Δq_p^a, Δq_j^b, Δq_p^c, Δq_p^d being presented in terms of components both of body forces $\{\bar{f}\}$ and contact forces $\{\bar{t}\}$ derived from preceding iterations.

It is seen that contact conditions in this procedure are conventional boundary conditions in displacements and forces for the modified system (46). A part of contact conditions (continuity of displacements $\Delta\tilde{u}_p^- = 0$ and forces $\Delta\tilde{q}_p^+ = \Delta q_p^a$ when crossing the contact boundary) is satisfied exactly at each iteration, another part of contact conditions (determination of their types and fulfilment of the slipping conditions) are determined by iteration. The above procedure is presented in Fig. 2.

3.3. A procedure for solving contact thermoelastoplastic problems at small and large strains

Thermoelastoplastic and contact elastic problems at small and large strains are non-linear, and they are solved by iteration. To construct a solution of a contact thermoelastoplastic problem one should combine the above iteration procedures. This may be performed by the algorithm seen in Fig. 3. Here, the thermoelastoplastic problem is solved by the algorithm (32) but having both a modified matrix $[\tilde{K}]$ instead of $[K]$ and variables $\{\Delta\tilde{u}\}$ and $\{\Delta\tilde{q}\}$.

It should be noted that another iteration procedure may be used: at first, the contact thermoelastic problem is solved, and then we use the algorithm presented in Fig. 3 (i.e. the initial approximation for the solving of the thermoelastoplastic problem is taken with account of slipping value derived when solving the contact thermoelastic problem). A numerical experiment has shown that in small loading steps a final solution is independent of the type of the algorithm used. This may be numerical evidence

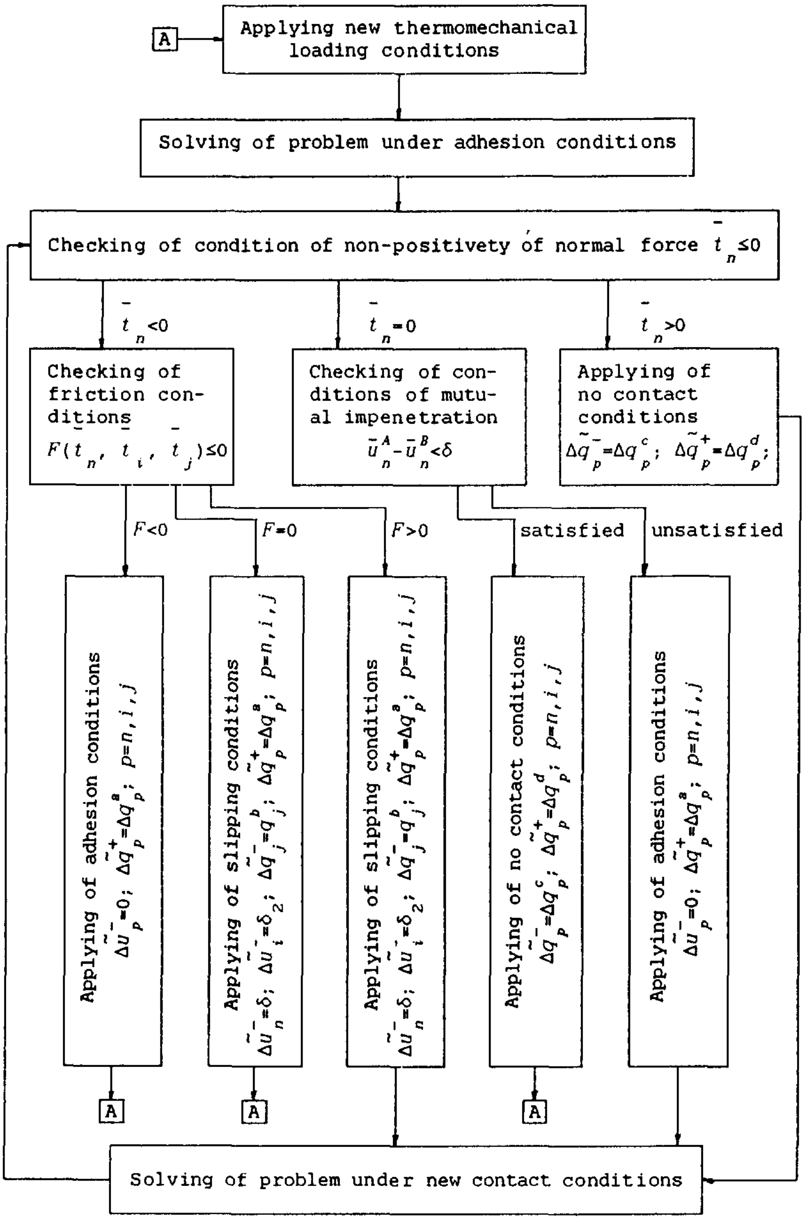

Fig. 2. Iterative procedure for applying contact conditions.

of convergence and uniqueness of a solution. It should be noted that the first procedure requires less computer time.

REMARK. The paper does not include theoretical evidence of convergence and uniqueness of a solution. This problem remains open.

The algorithm shown in Fig. 3 can be used both for small and large strains. We explain the fact using as an example the stepwise solution of a contact elastic problem at large strains. At first, one should solve elastic problem with adhesion conditions at contact boundary. In this case a modified matrix $[\tilde{K}]$ is used which can be calculated using a constant or tangential stiffness matrix. Then, contact conditions are checked and redetermined (as described above in Section 3.2). Further, an elastic problem at large strains and under new boundary conditions and new matrix $[\tilde{K}]$ is solved, and so on (see Fig. 3).

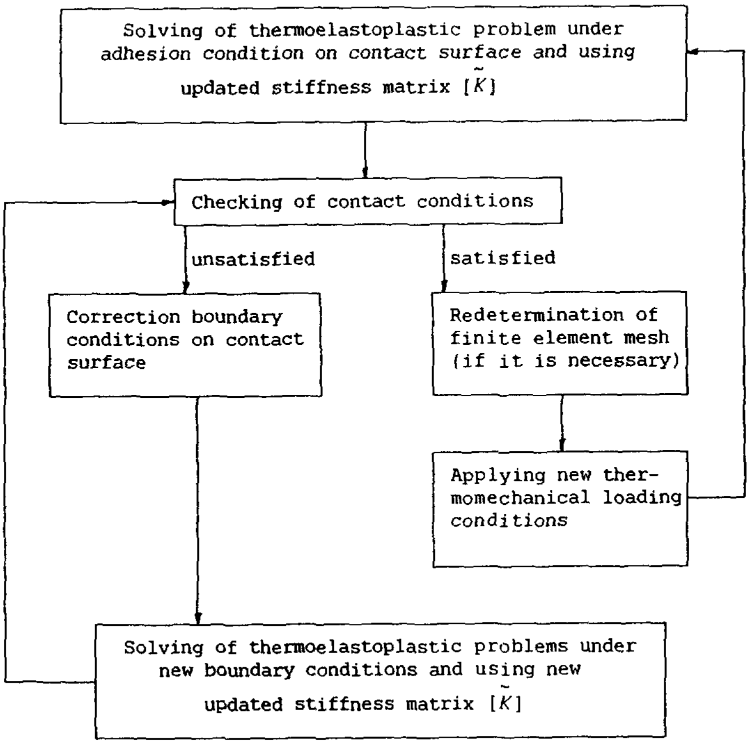

Fig. 3. An algorithm for solving contact thermoelastic problems.

4. Numerical examples

The developed technique for solving contact thermoelastoplastic problems at large strains has been implemented for an axisymmetric case as software by using the following effective methods: the stiffness matrix is stored in unidimensional array in columns; a blockwise structure of the formation and solution of a system of algebraic equations by direct LDL^t—factorization method has been developed. A number of testing examples at small and large strains as well as problems on stress–strain state (SSS) of components of high pressure apparatus (HPA) for superhard materials synthesis have been solved. All the problems stated below used axisymmetric linear triangular finite elements.

4.1. Problem on pressing the matrix into a ring unit

Fig. 4 shows a FE mesh of the matrix IV and rings I, II and III. These structural elements are used in high pressure apparatus to synthesize superhard materials. The assembly sequence is as follows: ring II is pressed into ring I, ring III is pressed into a unit of rings I, II, matrix IV is pressed into a unit of rings

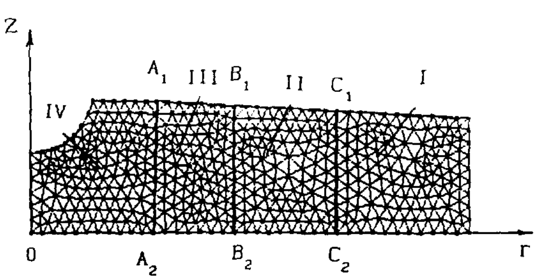

Fig. 4. Finite element mesh for matrix IV and rings I, II, III (523 nodes, 887 finite elements, 32 pairs of the interacting contact nodes).

I, II, III, the interference being $\delta_1 = 0.015$, $\delta_2 = 0.02$ and $\delta_3 = 0.02$, respectively. Thus, the solution of the complete problem reduces to the sequential solution of three problems which are defined by the order of the matrix and rings assembly. All contact surfaces A_1A_2, B_1B_2, C_1C_2 are conical, cone angle $\beta = 0.0334$. The problems are considered in an elastic formulation and for the case of small strains. The following mechanical properties were given: for the rings—Young's modulus $E = 2.1 \cdot 10^6$, Poisson's ratio $\nu = 0.3$; for the matrix—$E = 6.4 \cdot 10^6$, $\nu = 0.22$. Along C_1C_2, B_1B_2 interfaces the friction coefficient γ was given to be 0.15, along A_1A_2 interface—$\gamma = 0.1$. Fig. 5 shows variation of radial stresses σ_r along A_1A_2 contact surface. It should be noted that the numerical solution obtained differs from the analytical solution of the Lame's problem on pressing cylinders. This is mainly associated with account of friction forces as well as with non-cylindrical shape of the matrix IV.

REMARK. Each of the three problems on pressing the rings and the matrix was solved in one step of loading (at the contact surface according to the above procedure, the interference is directly given). Hypothetically, this corresponds to the following type of assembling: e.g. an outer ring (ring unit) is heated, it expands, and an inner ring (matrix) is easily inserted in it, then the construction is allowed to cool down to the initial temperature. In [33], the solution of the similar problem but in an elastoplastic formulation and in the case when the inner ring is forced into the outer ring (remind that the contact surface is conical) is given and then the problem on the force relief is considered. Such an account of the assembling character of pressing [33] is needed because of the fact that the solution of friction problems depends on loading history.

4.2. Necking in a simple tension test

Fig. 6 shows an initial and deformed (30% elongation) FE meshes. % elongation (engineering strain) is defined as $100\% \cdot (L - L_0)/L_0$, where L is the current length and L_0 is the initial length of the bar. The case of large strains (normal pressure) is considered. The following mechanical properties were given: $E = 30 \cdot 10^6$, $\nu = 0.333$, the loading surface was described by the relation $\sigma_i = 120(q + 0.0039)^{0.125}$, where q is the accumulated strain. The problem was solved in 30 steps of loading (displacement increments). The development of a neck as a function of elongation is show in Fig. 7. The results agree with data in [13].

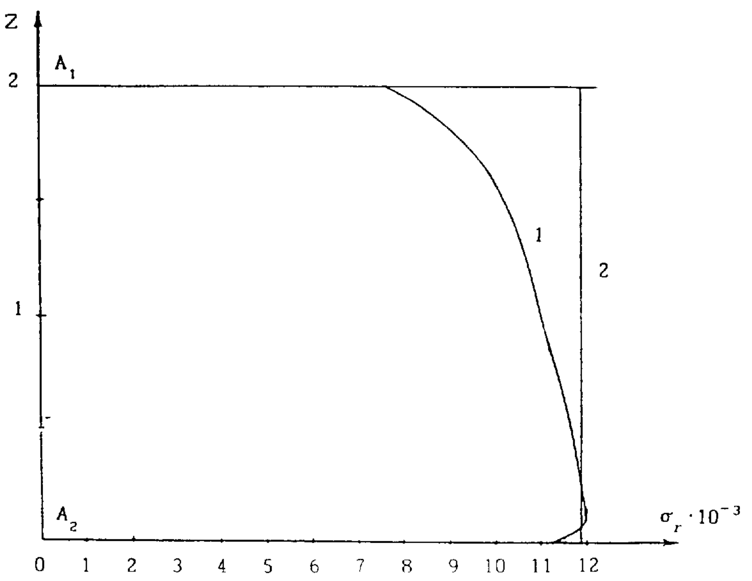

Fig. 5. Radial stresses distribution σ_r along A_1A_2 contact surface. 1—numerical solution, 2—analytical solution for Lame's problem.

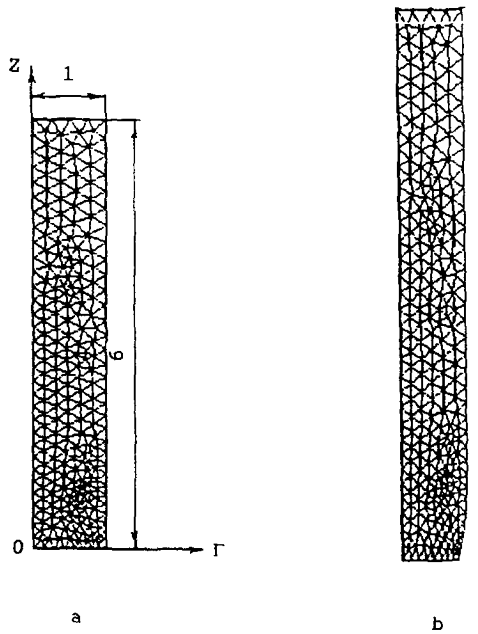

Fig. 6. (a) An initial mesh for a uniaxial tension test (266 nodes, 454 finite elements). (b) The deformed mesh at 30% elongation.

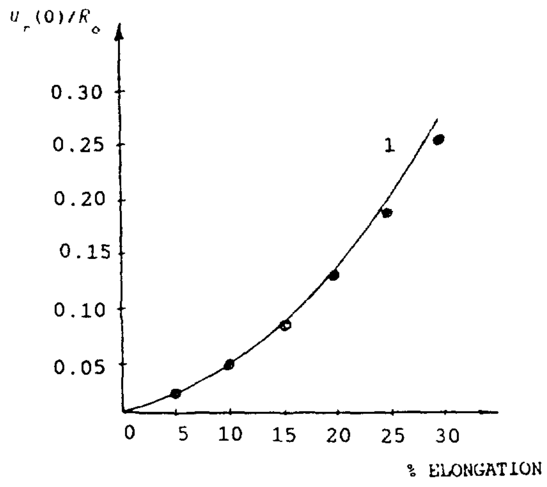

Fig. 7. Development of neck as a function of % elongation; $u_r(0)$—radial displacement at neck, R—initial radius. 1—numerical solution; ●—known numerical solution [13].

4.3. Stress–strain state of components of high pressure apparatus for synthesis of superhard materials

Consider, in short, the solution of a complex process problem on the determination of SSS of recessed-anvil type high pressure apparatus (HPA) for the production of superhard materials allowing for large strains, high pressures and temperatures, contact interaction. Fig. 8 shows the upper half of axial section of the HPA components, where $0r$ is the horizontal axis of symmetry, $0z$ is the axis of rotation (the components include elastic tungsten carbide matrix V and reaction mixture I, heater IV, container II, deformable gasket (DG) III, whose materials belong to a class of rocks and undergo elastoplastic deformation under high pressures). Coulumb's friction conditions were specified at the ABC surface. The following technological stages are considered in succession: (a) the compression with a force at the surface DK (the forces distributed over the surface KC are due to pressing of the matrix into a ring unit, the solution of this problem has considered above), see Fig. 9(a); (b) the redistribution

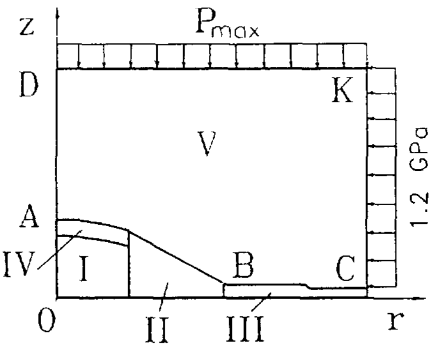

Fig. 8. The cross-section of components of high pressure apparatus.

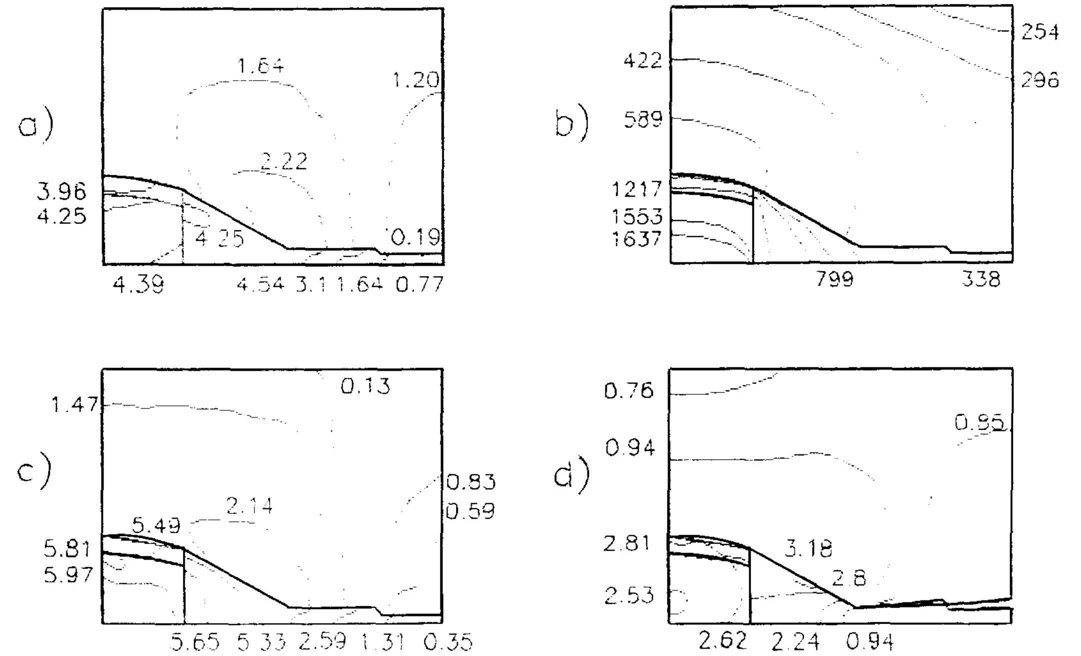

Fig. 9. The pressure distribution (GPa) in the HPA components when compressed (a), heated (c) and unloaded (d) (at $P = 0.24$ P_{max}, P_{max} is the maximum force) and the temperature distribution (°C) in the HPA (b) components.

of stresses due to heating, see Fig. 9(c); and (c) the unloading which includes cooling and force-relieving on the surface DK, see Fig. 9(d) (at a force of $P = 0.24$ P_{max} a gap forms between the matrix and DG).

Note that under compression we redetermined the FE mesh four times. The criterion of redetermination of the FE mesh was of two conditions: (a) the angles of triangular FE after deformation should not be less than ε ($\varepsilon = 15°$–$20°$); (b) the coordinates of the interacting contact nodes at the ABC surface should not differ more than 0.1–0.2 l, l—the length of a side of corresponding triangular FE (parameters ε and l were determined from numerical experiments). The meshes of HPA components included 1078–1269 nodes and 1904–2186 FE, 58–68 pairs of contact nodes.

Let us analyze the calculation results. Under compression, maximum values of accumulated plastic strain (in DG) are 80 to 100%, maximum volumetric elastic strains (in the mixture) are 7 to 9%. The calculated integral compressive force-vs-displacement curve shows good agreement with the experimental one. A satisfactory agreement between stress values for the DG calculated using FEM and slip-line method [1, 2] is obtained.

To calculate the stage of heating, a non-steady temperature field was used which resulted from the solution of a coupled non-linear non-steady electrical conductivity problem [34]. Non-steady temperature field and fields of stresses and strains in compression were used as initial data to calculate SSS in heating. Calculation results obtained showed monotonous increase of pressure in the reaction mixture, and in the case of steady-temperature field (Fig. 9(b), maximum temperature of 1637°C is in the central region of the mixture) the pressure increment attains ca. 41%, this agrees with known experimental data, light thinning of DG being observed, this agrees with the experiment as well. To study the effect of temperature dependence of mechanical properties on SSS of HPA components, the stage of heating was calculated without regard for temperature dependence of mechanical properties, when heating effect was taken into account only in terms of thermal expansion coefficient. In this case pressure increment in the reaction mixture amounted to 59%, i.e. the effect of temperature on properties of materials for HPA components must not be ignored.

The unloading stage consists of two processes: cooling and force unloading as such. SSS in heating and non-steady temperature field in cooling which resulted from the solution of a non-steady non-linear electrical conductivity problem [34] were used as the initial data to calculate the SSS of HPA components in cooling. From the solution of a cooling problem, changes in SSS are defined and pressure drop down to 4.1–4.3 GPa is found in the reaction mixture. The initial data (to calculate SSS in force relieving) are stresses and strains achieved in cooling. It is found from the solution of an unloading problem that a 51% (and more) reduction in compressive force results in decrease of the matrix/DG contact boundary and at the compressive force of 0.24 P_{max} (P_{max} is the maximum compressive force) a gap is formed between them (Fig. 9(d)), pressure in the reaction mixture being rather high (2.5–2.6 GPa). That can cause failure to the container.

The results obtained are used for simulating diamond synthesis and evaluating strength and durability of the HPA matrices.

5. Conclusion

The present work offers a numerical procedure to solve contact thermoelastoplastic problems at large strains, normal and high pressures and temperatures.

The main features of the procedure are as follows:

(a) A rigorous derivation of the constitutive relations is given, large volumetric elastic and temperature deformations are properly correctly accounted for. Considered are the likely ways for the concretization of the elastic law at high pressures.

(b) The procedure for solving thermoelastoplastic problems at large strains differs only slightly from the case of small strains, this makes it convenient in practical realization.

(c) The procedure of solving contact problems for deformable bodies allows reduction of the contact interaction conditions to usual boundary conditions in displacements and stresses for the modified FE system of algebraic equations with symmetrical stiffness matrix. And a part of contact conditions (continuity of displacements and stresses when crossing the contact boundary) are exactly satisfied, while another part of conditions (determination of type of contact conditions in pairs of contact nodes—adhesion, slipping, no-contact state and satisfying the slipping conditions) are satisfied by constructing an iterative procedure. This algorithm is easily realized for an arbitrary number of the contacting bodies having intricate contact boundaries, and converges rather well.

(d) Two iteration procedures are proposed for taking into account the contact interaction and plastic flow. Using a numerical experiment, one has shown their equivalence and has chosen the more optimal one from the standpoint of computer aided calculation time.

(e) The procedure proposed has been realized for an axisymmetric case as software. Testing problems as well as problems on stress–strain state of elements of HPA for synthesis of superhard materials have been solved with due account of large strains, high pressures and temperature, and contact interaction. The mechanism of HPA elements deformation have been determined, and a good correlation with experimental data has been obtained. Thus, the developed procedure has shown itself as an efficient way for solving complex problems of mechanics.

Acknowledgment

The financial support of Alexander von Humboldt Foundation for V.I.L. is gratefully acknowledged.

Appendix A. Derivation of kinematic relations

Let us shortly describe the derivation made in [1, 2]. According to [1, 2] we consider first, the no-thermal strain case ($\boldsymbol{U}_\theta = \boldsymbol{I}$—unit tensor). Then, Eq. (1) can be rewritten

$$\boldsymbol{F} = \boldsymbol{V}_e \cdot \boldsymbol{V}_p \cdot \boldsymbol{R}_e\,, \tag{A.1}$$

where

$$\boldsymbol{V}_p = \boldsymbol{R}_e \cdot \boldsymbol{U}_p \cdot \boldsymbol{R}_e^t\,.$$

Velocity gradient $\boldsymbol{l}$ and deformation rate $\boldsymbol{d}$ are described as

$$\begin{aligned}\boldsymbol{l} &= \frac{\partial \boldsymbol{v}}{\partial \boldsymbol{x}} = \dot{\boldsymbol{F}} \cdot \boldsymbol{F}^{-1} = (\overline{\boldsymbol{V}_e \cdot \boldsymbol{V}_p \cdot \boldsymbol{R}_e})^{\cdot} \cdot \boldsymbol{R}_e^t \cdot \boldsymbol{V}_p^{-1} \cdot \boldsymbol{V}_e^{-1} \\ &= \dot{\boldsymbol{V}}_e \cdot \boldsymbol{V}_e^{-1} + \boldsymbol{V}_e \cdot \dot{\boldsymbol{V}}_p \cdot \boldsymbol{V}_p^{-1} \cdot \boldsymbol{V}_e^{-1} + \boldsymbol{V}_e \cdot \boldsymbol{V}_p \cdot (\dot{\boldsymbol{R}}_e \cdot \boldsymbol{R}_e^t) \cdot \boldsymbol{V}_p^{-1} \cdot \boldsymbol{V}_e^{-1} \\ &= \dot{\boldsymbol{V}}_e \cdot \boldsymbol{V}_e^{-1} + \boldsymbol{V}_e \cdot (\dot{\boldsymbol{V}}_p + \boldsymbol{V}_p \cdot \boldsymbol{\Omega}_e + \boldsymbol{\Omega}_e^t \cdot \boldsymbol{V}_p - \boldsymbol{\Omega}_e^t \cdot \boldsymbol{V}_p) \cdot \boldsymbol{V}_p^{-1} \cdot \boldsymbol{V}_e^{-1} \\ &= (\dot{\boldsymbol{V}}_e \cdot \boldsymbol{V}_e^{-1} + \boldsymbol{V}_e \cdot \boldsymbol{\Omega}_e \cdot \boldsymbol{V}_e^{-1}) + \boldsymbol{V}_e \cdot (\overset{\circ}{\boldsymbol{V}}_p \cdot \boldsymbol{V}_p^{-1}) \cdot \boldsymbol{V}_e^{-1}\,,\end{aligned} \tag{A.2}$$

$$\boldsymbol{d} = (\boldsymbol{l})_s = (\dot{\boldsymbol{V}}_e \cdot \boldsymbol{V}_e^{-1})_s + (\boldsymbol{V}_e \cdot \boldsymbol{\Omega}_e \cdot \boldsymbol{V}_e^{-1})_s + (\boldsymbol{V}_e \cdot \overset{\circ}{\boldsymbol{V}}_p \cdot \boldsymbol{V}_p^{-1} \cdot \boldsymbol{V}_e^{-1})_s\,, \tag{A.3}$$

where $\boldsymbol{v} = \dot{\boldsymbol{x}}$ is the velocity vector, $\boldsymbol{\Omega}_e$ is the antisymmetrical tensor of an elastic spin, $\boldsymbol{\Omega}_e = \dot{\boldsymbol{R}}_e \cdot \boldsymbol{R}_e^t = -\boldsymbol{\Omega}_e^t$; $\overset{\circ}{\boldsymbol{V}}_p = \dot{\boldsymbol{V}}_p + \boldsymbol{V}_p \cdot \boldsymbol{\Omega}_e + \boldsymbol{\Omega}_e^t \cdot \boldsymbol{V}_p$ is the objective $\boldsymbol{R}$-derivative. Let us transform the expression $(\dot{\boldsymbol{V}}_e \cdot \boldsymbol{V}_e^{-1})_s$.

$$\begin{aligned}(\dot{\boldsymbol{V}}_e \cdot \boldsymbol{V}_e^{-1})_s &= \boldsymbol{V}_e^{-1} \cdot (\dot{\boldsymbol{V}}_e \cdot \boldsymbol{V}_e)_s \cdot \boldsymbol{V}_e^{-1} = \frac{1}{2} \boldsymbol{V}_e^{-1} \cdot (\overline{\boldsymbol{V}_e \cdot \boldsymbol{V}_e})^{\cdot} \cdot \boldsymbol{V}_e^{-1} \\ &= \frac{1}{2} \boldsymbol{V}_e^{-1} \cdot (\overline{\boldsymbol{V}_e \cdot \boldsymbol{V}_e - \boldsymbol{I}})^{\cdot} \cdot \boldsymbol{V}_e^{-1} = \boldsymbol{V}_e^{-1} \cdot \dot{\boldsymbol{B}}_e \cdot \boldsymbol{V}_e^{-1}\,,\end{aligned} \tag{A.4}$$

where

$$\boldsymbol{B}_e = \frac{1}{2}(\boldsymbol{V}_e \cdot \boldsymbol{V}_e - \boldsymbol{I}) = \frac{1}{2}(\boldsymbol{F}_e \cdot \boldsymbol{F}_e^t - \boldsymbol{I})\,. \tag{A.5}$$

Similarly,

$$\begin{aligned}(\boldsymbol{V}_e \cdot \boldsymbol{\Omega}_e \cdot \boldsymbol{V}_e^{-1})_s &= \frac{1}{2} \boldsymbol{V}_e^{-1} \cdot (\boldsymbol{V}_e \cdot \boldsymbol{V}_e \cdot \boldsymbol{\Omega}_e + \boldsymbol{\Omega}_e^t \cdot \boldsymbol{V}_e \cdot \boldsymbol{V}_e) \cdot \boldsymbol{V}_e^{-1} \\ &= \frac{1}{2} \boldsymbol{V}_e^{-1} \cdot [(\boldsymbol{V}_e \cdot \boldsymbol{V}_e - \boldsymbol{I}) \cdot \boldsymbol{\Omega}_e + \boldsymbol{\Omega}_e^t \cdot (\boldsymbol{V}_e \cdot \boldsymbol{V}_e - \boldsymbol{I})] \cdot \boldsymbol{V}_e^{-1} \\ &= \boldsymbol{V}_e^{-1} \cdot (\boldsymbol{B}_e \cdot \boldsymbol{\Omega}_e + \boldsymbol{\Omega}_e^t \cdot \boldsymbol{B}_e) \cdot \boldsymbol{V}_e^{-1}\,.\end{aligned} \tag{A.6}$$

As $\dot{\boldsymbol{B}}_e + \boldsymbol{B}_e \cdot \boldsymbol{\Omega}_e + \boldsymbol{\Omega}_e^t \cdot \boldsymbol{B}_e = \overset{\circ}{\boldsymbol{B}}_e$, then

$$\boldsymbol{d} = \boldsymbol{V}_e^{-1} \cdot \overset{\circ}{\boldsymbol{B}}_e \cdot \boldsymbol{V}_e^{-1} + (\boldsymbol{V}_e \cdot \overset{\circ}{\boldsymbol{V}}_p \cdot \boldsymbol{V}_p^{-1} \cdot \boldsymbol{V}_e^{-1})_s\,. \tag{A.7}$$

Tensor $\boldsymbol{\Omega}_e$ is easily determined from the equation

$$(\boldsymbol{V}_e \cdot \boldsymbol{\Omega}_e)_a = (\boldsymbol{l} \cdot \boldsymbol{V}_e)_a - (\boldsymbol{V}_e \cdot \overset{\circ}{\boldsymbol{V}}_p \cdot \boldsymbol{V}_p^{-1})_a\,, \tag{A.8}$$

which is derived from Eq. (A.2) and does not contain $\dot{\boldsymbol{V}}_e$.

Let the volumetric elastic strains be finite, and the shear strains—small, i.e. $\boldsymbol{V}_e = a\boldsymbol{I} + \boldsymbol{\varepsilon}$, $\varepsilon_{ij} \ll 1$, where $\boldsymbol{\varepsilon}$ is the deviator. Then

$$\boldsymbol{V}_e^{-1} = \frac{1}{a}\boldsymbol{I} + \frac{1}{a^2}\boldsymbol{\varepsilon}\,, \qquad \boldsymbol{B}_e = \frac{a^2-1}{2}\boldsymbol{I} + \boldsymbol{\varepsilon}\,.$$

It follows from Eq. (A.2) that the tensor of $\boldsymbol{W}$ vortex

$$\boldsymbol{W} \stackrel{\text{def}}{=} (\boldsymbol{l})_a = \frac{1}{a^2}(\dot{\boldsymbol{V}}_e \cdot \boldsymbol{\varepsilon})_a + \boldsymbol{\Omega}_e + (\overset{\circ}{\boldsymbol{V}}_p \cdot \boldsymbol{V}_p^{-1})_a\,. \tag{A.9}$$

Having determined $\boldsymbol{\Omega}_e$ from Eq. (A.9) and substituted it into Eq. (A.7) we obtain

$$\boldsymbol{d} = \frac{1}{a^2}\overset{\nabla}{\boldsymbol{B}}_e + \boldsymbol{d}_p\,, \tag{A.10}$$

where $\boldsymbol{d}_p = (\overset{\circ}{\boldsymbol{V}}_p \cdot \boldsymbol{V}_p^{-1})_s$ is the tensor of the plastic deformation rate, $\overset{\nabla}{\boldsymbol{B}}_e = \dot{\boldsymbol{B}}_e + 2(\boldsymbol{B}_e \cdot \boldsymbol{W})_s$ is the Jaumann derivative of $\boldsymbol{B}_e$ tensor. When deriving (A.10) we have used that

$$[\boldsymbol{B}_e \cdot (\overset{\circ}{\boldsymbol{V}}_p \cdot \boldsymbol{V}_p^{-1})_a]_s = [\boldsymbol{\varepsilon} \cdot (\overset{\circ}{\boldsymbol{V}}_p \cdot \boldsymbol{V}_p^{-1})_a]_s \ll (\overset{\circ}{\boldsymbol{V}}_p \cdot \boldsymbol{V}_p^{-1})_s\,,$$

$$\left[\boldsymbol{B}_e \cdot \frac{1}{a^2}(\dot{\boldsymbol{V}}_e \cdot \boldsymbol{\varepsilon})_a\right]_s = \frac{1}{a^2}[\boldsymbol{\varepsilon} \cdot (\dot{\boldsymbol{V}}_e \cdot \boldsymbol{\varepsilon})_a]_s \ll \dot{\boldsymbol{B}}_e = a\dot{\boldsymbol{V}}_e\,.$$

To account for the thermal deformations $\boldsymbol{U}_\theta = (\alpha\theta + 1)\boldsymbol{I}$ we assume that the thermoelastic left stretch tensor is $\boldsymbol{V}_{e\theta} = \boldsymbol{V}_e \cdot \boldsymbol{U}_\theta$. Then, Eq. (A.1) is rewritten in the form

$$\boldsymbol{F} = \boldsymbol{V}_{e\theta} \cdot \boldsymbol{V}_p \cdot \boldsymbol{R}_e\,. \tag{A.11}$$

Assuming that

$$\boldsymbol{B}_{e\theta} = \frac{1}{2}(\boldsymbol{V}_{e\theta} \cdot \boldsymbol{V}_{e\theta} - \boldsymbol{I}) = \frac{1}{2}[(\alpha\theta + 1)^2\boldsymbol{V}_e \cdot \boldsymbol{V}_e - \boldsymbol{I}] = \frac{1}{2}[(\alpha\theta + 1)^2(2\boldsymbol{B}_e + \boldsymbol{I}) - \boldsymbol{I}] \tag{A.12}$$

and accounting for that

$$\boldsymbol{V}_{e\theta} = (\alpha\theta + 1)a\boldsymbol{I} + \boldsymbol{\varepsilon}\,, \qquad \overset{\nabla}{\boldsymbol{B}}_{e\theta} = (\alpha\theta + 1)^2\overset{\nabla}{\boldsymbol{B}}_e = \frac{a^2}{2}\dot{\overline{(\alpha\theta + 1)^2}}\boldsymbol{I}\,, \qquad (\boldsymbol{B}_{e\theta} \cdot \boldsymbol{W})_s = (\alpha\theta + 1)^2(\boldsymbol{B}_e \cdot \boldsymbol{W})_s\,,$$

as in the case with deriving Eq. (A.10) we get

$$\begin{aligned} \boldsymbol{d} &= \frac{(\alpha\theta + 1)^2\overset{\nabla}{\boldsymbol{B}}_e + \frac{a^2}{2}\dot{\overline{(\alpha\theta + 1)^2}}\boldsymbol{I}}{(\alpha\theta + 1)^2a^2} + \boldsymbol{d}_p = \frac{\overset{\nabla}{\boldsymbol{B}}_e}{a^2} + \frac{1}{2}\frac{\dot{\overline{(\alpha\theta + 1)^2}}}{(\alpha\theta + 1)^2}\boldsymbol{I} + \boldsymbol{d}_p \\ &= \frac{\overset{\nabla}{\boldsymbol{B}}_e}{a^2} + \frac{\dot{\overline{\alpha\theta}}}{(1 + \alpha\theta)}\boldsymbol{I} + \boldsymbol{d}_p\,, \end{aligned} \tag{A.13}$$

$$a^2 = \frac{2}{3}I_1(\boldsymbol{B}_e) + 1\,.$$

At small volumetric elastic strains in Eq. (A.13) one should assume $a^2 = 1$, at small thermal deformations $1 + \alpha\theta \approx 1$. It should be noted that for the case of isotropic material analyzed in the paper, there is no necessity for the calculation of $\boldsymbol{\Omega}_e$, $\overset{\circ}{\boldsymbol{V}}_p$ and $\boldsymbol{V}_p$, as the model includes only the rate of plastic deformation $\boldsymbol{d}_p$and the accumulated plastic strain q which is determined by means of it.

Appendix B. Feasible ways for the concretization of the thermoelastic law at high pressures

Let us consider in detail the isotropic law of thermoelasticity under high pressure (9) and feasible ways for its concretization for the case when shear elastic strains are small as compared with unity. In the general case the isotropic elastic law is presented in the form [35]

$$\boldsymbol{T}=\frac{1}{\sqrt{I_3(\boldsymbol{P})}}(\Psi_0\boldsymbol{I}+\Psi_1\boldsymbol{P}+\Psi_2\boldsymbol{P}^2)\,, \tag{B.1}$$

where $\boldsymbol{P}=\boldsymbol{F}_e\cdot\boldsymbol{F}_e^t=\boldsymbol{B}_e+\boldsymbol{I}$ is the left Cauchy–Green tensor of deformation, Ψ_0, Ψ_1, Ψ_2 are the functions of I_1, I_2, I_3 invariants of $\boldsymbol{P}$ tensor. Potentiality conditions for hyperelasic material (under the assumption that there exists an elastic potential at large elastic strains) impose additional constraints on Ψ_0, Ψ_1 and Ψ_2, one of which is [35]

$$I_3\frac{\partial}{\partial I_3}(\Psi_1+I_1\Psi_2)=\frac{\partial\Psi_0}{\partial I_1}\,. \tag{B.2}$$

In case of small shear strains the elastic law is taken in the form of a quasilinear dependence of $\boldsymbol{T}$ stresses on $\boldsymbol{B}_e$ tensor

$$\boldsymbol{T}=[f_1(I_1)+f_2(I_1)]\boldsymbol{I}+2f_2(I_1)\boldsymbol{B}_e\,, \tag{B.3}$$

where f_1 and f_2 are certain functions of the first invariant $I_1(\boldsymbol{B}_e)$ of the tensor $\boldsymbol{B}_e$. Comparison between Eqs. (B.1) and (B.3) yields

$$f_1(I_1(\boldsymbol{B}_e))=\frac{\Psi_0}{\sqrt{I_3(\boldsymbol{P})}}\,,\qquad f_2(I_1(\boldsymbol{B}_e))=\frac{\Psi_1}{\sqrt{I_3(\boldsymbol{P})}}\,,\quad \Psi_2\equiv 0\,. \tag{B.4}$$

Taking into account that $I_1(\boldsymbol{P})=2I_1(\boldsymbol{B}_e)+3$ and $\partial/\partial I_1(\boldsymbol{P})=\frac{1}{2}\,\partial/\partial I_1(\boldsymbol{B}_e)$, from Eq. (B.2) we have

$$f_2(I_1)=\frac{\partial f_1(I_1)}{\partial I_1}\,. \tag{B.5}$$

Then, Eq. (B.3) can be written in the form

$$\boldsymbol{T}=\left[f_1(I_1)+\frac{\partial f_1(I_1)}{\partial I_1}\right]\boldsymbol{I}+2\frac{\partial f_1}{\partial I_1}\boldsymbol{B}_e\,. \tag{B.6}$$

It is assumed that when $\boldsymbol{B}_e=0$, stress tensor $\boldsymbol{T}=0$, i.e.

$$\left[[f_1(I_1)+\frac{\partial f_1(I_1)}{\partial I_1}\right]\Bigg|_{I_1=0}=0\,. \tag{B.7}$$

Let us consider polynomial approximations of the function $f_1=f_1(I_1)$. Let f_1 be the polynomial of the second power

$$f_1=A+BI_1+CI_1^2\,,\quad A,B,C=\text{const}\,. \tag{B.8}$$

Then, from Eqs. (B.6) and (B.7) we have that the elastic law (B.3) can be rewritten in the form

$$\boldsymbol{T}=[(2C-A)I_1+CI_1^2]\boldsymbol{I}-2(-A+2CI_1)\boldsymbol{B}_e=\left[\lambda I_1+\frac{1}{2}(\lambda-\mu)I_1^2\right]\boldsymbol{I}+2[\mu+(\lambda-\mu)I_1]\boldsymbol{B}_e\,, \tag{B.9}$$

where $\lambda=2C-\mu$, $\mu=-A$ is the Lame constants which are found in experiments at small strains.

Let f_1 be the polynomial of the third power

$$f_1=A+BI_1+CI_1^2+DI_1^3\,,\quad A,B,C,D=\text{const}\,. \tag{B.10}$$

By analogy (B.9) we can show that

$$\boldsymbol{T}=\left[\lambda I_1+\frac{1}{2}(\lambda-\mu+6D)I_1^2+DI_1^3\right]\boldsymbol{I}+2[\mu+(\lambda-\mu)I_1+3DI_1^2]\boldsymbol{B}_e\,, \tag{B.11}$$

where λ, μ are the Lame constant which are found in experiments at small strains, and the constant D must be found in any experiment at large strains.

For the thermoelastic law, in relations (B.3)–(B.11), one should assume that $f_1 = f_1(I_1, \theta)$, $f_2 = f_2(I_1, \theta)$, $A = A(\theta)$, $B = B(\theta)$, $C = C(\theta)$, $D = D(\theta)$.

Appendix C. Derivation of the thermoelastoplastic rate equations

Let us write the elastic law (9) in the rate form

$$\overset{\nabla}{\boldsymbol{T}} = \dot{\boldsymbol{T}} + \boldsymbol{T}\cdot\boldsymbol{W} + \boldsymbol{W}^{\mathrm{t}}\cdot\boldsymbol{T} = (\dot{\boldsymbol{E}}:\boldsymbol{B}_{\mathrm{e}} + \boldsymbol{E}:\dot{\boldsymbol{B}}_{\mathrm{e}}) + (\boldsymbol{E}:\boldsymbol{B}_{\mathrm{e}})\cdot\boldsymbol{W} + \boldsymbol{W}^{\mathrm{t}}\cdot(\boldsymbol{E}:\boldsymbol{B}_{\mathrm{e}}) . \tag{C.1}$$

A direct substitution makes us sure that

$$\begin{aligned}(\boldsymbol{E}:\boldsymbol{B}_{\mathrm{e}})\cdot\boldsymbol{W} + \boldsymbol{W}^{\mathrm{t}}\cdot(\boldsymbol{E}:\boldsymbol{B}_{\mathrm{e}}) &= \lambda I_1(\boldsymbol{B}_{\mathrm{e}})\boldsymbol{W} + 2\mu\boldsymbol{B}_{\mathrm{e}}\cdot\boldsymbol{W} + \lambda I_1(\boldsymbol{B}_{\mathrm{e}})\boldsymbol{W}^{\mathrm{t}} + 2\mu\boldsymbol{W}^{\mathrm{t}}\cdot\boldsymbol{B}_{\mathrm{e}}\\ &= 2\mu\boldsymbol{B}_{\mathrm{e}}\cdot\boldsymbol{W} + 2\mu\boldsymbol{W}^{\mathrm{t}}\cdot\boldsymbol{B}_{\mathrm{e}}\\ &= (\lambda I_1(\boldsymbol{B}_{\mathrm{e}}\cdot\boldsymbol{W})\boldsymbol{I} + 2\mu\boldsymbol{B}_{\mathrm{e}}\cdot\boldsymbol{W}) + (\lambda I_1(\boldsymbol{W}^{\mathrm{t}}\cdot\boldsymbol{B}_{\mathrm{e}})\boldsymbol{I} + \boldsymbol{W}^{\mathrm{t}}\cdot\boldsymbol{B}_{\mathrm{e}})\\ &= \boldsymbol{E}:(\boldsymbol{B}_{\mathrm{e}}\cdot\boldsymbol{W}) + \boldsymbol{E}:(\boldsymbol{W}^{\mathrm{t}}\cdot\boldsymbol{B}_{\mathrm{e}}) .\end{aligned} \tag{C.2}$$

It is taken into account here that $I_1(\boldsymbol{B}_{\mathrm{e}}\cdot\boldsymbol{W}) = \boldsymbol{B}_{\mathrm{e}}:\boldsymbol{W} = 0$, $I_1(\boldsymbol{W}^{\mathrm{t}}\cdot\boldsymbol{B}_{\mathrm{e}}) = \boldsymbol{W}^{\mathrm{t}}:\boldsymbol{B}_{\mathrm{e}} = 0$, since $\boldsymbol{B}_{\mathrm{e}} = \boldsymbol{B}_{\mathrm{e}}^{\mathrm{t}}$, $\boldsymbol{W} = -\boldsymbol{W}^{\mathrm{t}}$. Then, it follows from Eq. (C.1) that

$$\overset{\nabla}{\boldsymbol{T}} = \dot{\boldsymbol{E}}:\boldsymbol{B}_{\mathrm{e}} + \boldsymbol{E}:(\dot{\boldsymbol{B}}_{\mathrm{e}} + \boldsymbol{B}_{\mathrm{e}}\cdot\boldsymbol{W} + \boldsymbol{W}^{\mathrm{t}}\cdot\boldsymbol{B}_{\mathrm{e}}) = \dot{\boldsymbol{E}}:\boldsymbol{B}_{\mathrm{e}} + \boldsymbol{E}:\overset{\nabla}{\boldsymbol{B}}_{\mathrm{e}} . \tag{C.3}$$

The plastic flow rule is taken in the form (14)

$$\boldsymbol{d}_{\mathrm{p}} = \lambda_1\boldsymbol{S} , \quad \lambda_1 \geqslant 0 , \tag{C.4}$$

where $\boldsymbol{S}$ is the stress deviator.

In the elastoplastic region

$$\varphi = \varphi(\boldsymbol{T}, q, \theta) = \sigma_i - \Phi(q, \theta)(1 + \kappa\sigma_0) = 0 \tag{C.5}$$

and

$$\dot{\varphi} = \frac{\partial\varphi}{\partial\boldsymbol{T}}:\dot{\boldsymbol{T}} + \frac{\partial\varphi}{\partial q}\dot{q} + \frac{\partial\varphi}{\partial\theta}\dot{\theta} = 0 . \tag{C.6}$$

Considering that

$$\frac{\partial\sigma_i}{\partial\boldsymbol{T}} = \frac{\boldsymbol{S}}{\sigma_i} , \qquad \frac{\partial\sigma_0}{\partial\boldsymbol{T}} = \frac{1}{3}\boldsymbol{I} , \qquad \frac{\partial\varphi}{\partial\boldsymbol{T}} = \frac{\boldsymbol{S}}{\sigma_i} - \frac{1}{3}\Phi(q, \theta)\kappa\boldsymbol{I} ,$$

one can show that $\partial\varphi/\partial\boldsymbol{T}:\overset{\nabla}{\boldsymbol{T}} = \partial\varphi/\partial\boldsymbol{T}:\dot{\boldsymbol{T}}$. Really,

$$\frac{\partial\varphi}{\partial\boldsymbol{T}}:\overset{\nabla}{\boldsymbol{T}} = \frac{\partial\varphi}{\partial\boldsymbol{T}}:(\dot{\boldsymbol{T}} + \boldsymbol{T}\cdot\boldsymbol{W} + \boldsymbol{W}^{\prime}\cdot\boldsymbol{T}) = \frac{\partial\varphi}{\partial\boldsymbol{T}}:\dot{\boldsymbol{T}} + \frac{\partial\varphi}{\partial\boldsymbol{T}}:(\boldsymbol{T}\cdot\boldsymbol{W}) + \frac{\partial\varphi}{\partial\boldsymbol{T}}:(\boldsymbol{W}^{\mathrm{t}}\cdot\boldsymbol{T}) ,$$

$$\begin{aligned}\frac{\partial\varphi}{\partial\boldsymbol{T}}:(\boldsymbol{T}\cdot\boldsymbol{W}) &= \left(\frac{\boldsymbol{S}}{\sigma_i} - \frac{1}{3}\Phi(q, \theta)\kappa\boldsymbol{I}\right):\left[\left(\boldsymbol{S} + \frac{1}{3}\sigma_0\boldsymbol{I}\right)\cdot\boldsymbol{W}\right]\\ &= \frac{\boldsymbol{S}\cdot\boldsymbol{S}:\boldsymbol{W}}{\sigma_i} - \frac{1}{3}\Phi(q, \theta)\kappa\boldsymbol{S}:\boldsymbol{W} + \frac{1}{3}\frac{\sigma_0}{\sigma_i}\boldsymbol{S}:\boldsymbol{W} - \frac{1}{9}\Phi(q, \theta)\kappa\sigma_0\boldsymbol{S}:\boldsymbol{W} = 0 ,\end{aligned}$$

as $(\boldsymbol{W}:\boldsymbol{b}) = 0$ for any symmetrical tensor $\boldsymbol{b}$. By analogy, $\partial\varphi/\partial\boldsymbol{T}:(\boldsymbol{W}^{\mathrm{t}}\cdot\boldsymbol{T}) = 0$. Thus,

$$\dot{\varphi} = \frac{\partial\varphi}{\partial\boldsymbol{T}}:\overset{\nabla}{\boldsymbol{T}} + \frac{\partial\varphi}{\partial q}\dot{q} + \frac{\partial\varphi}{\partial\theta}\dot{\theta} = 0 . \tag{C.7}$$

It follows from (2) that

$$\overset{\nabla}{\boldsymbol{B}}_{\mathrm{e}} = a^2(\boldsymbol{d} - \boldsymbol{d}_{\mathrm{p}} - \boldsymbol{d}_{\theta}) . \tag{C.8}$$

Substituting consecutively Eq. (C.4) into Eq. (C.8), Eq. (C.8) into Eq. (C.3), Eq. (C.3) into Eq. (C.7) and taking into account that $\dot{q} = (\frac{2}{3}\, \boldsymbol{d}_p : \boldsymbol{d}_p)^{1/2} = \lambda_1(\frac{2}{3}\, \boldsymbol{S} : \boldsymbol{S})^{1/2}$, we obtain

$$\lambda_1 = \frac{1}{\nu}\left[a^2 \frac{\partial \varphi}{\partial \boldsymbol{T}} : \dot{\boldsymbol{E}} : \boldsymbol{B}_e + \frac{\partial \varphi}{\partial \theta}\,\dot{\theta} + a^2 \frac{\partial \varphi}{\partial \boldsymbol{T}} : \boldsymbol{E} : (\boldsymbol{d} - \boldsymbol{d}_\theta)\right], \tag{C.9}$$

$$\nu = a^2 \frac{\partial \varphi}{\partial \boldsymbol{T}} : \boldsymbol{E} : \boldsymbol{S} - \frac{\partial \varphi}{\partial q}\left(\frac{2}{3}\boldsymbol{S} : \boldsymbol{S}\right)^{1/2},$$

$$\dot{\boldsymbol{E}} = \frac{\partial \boldsymbol{E}}{\partial I_1(\boldsymbol{B}_e)}\, \dot{I}_1(\boldsymbol{B}_e) + \frac{\partial \boldsymbol{E}}{\partial \theta}\,\dot{\theta} = a^2 \frac{\partial \boldsymbol{E}}{\partial I_1(\boldsymbol{B}_e)}\,[\boldsymbol{I} : (\boldsymbol{d} - \boldsymbol{d}_\theta)] + \frac{\partial \boldsymbol{E}}{\partial \theta}\,\dot{\theta}\,.$$

Substituting Eq. (C.4) into Eq. (C.8), Eq. (C.8) into Eq. (C.3) and taking account of Eq. (C.9), we obtain the required expression

$$\overset{\nabla}{\boldsymbol{T}} = \left(\boldsymbol{E} - \frac{a^2}{\nu}\boldsymbol{E} : \boldsymbol{S}\frac{\partial \varphi}{\partial \boldsymbol{T}} : \boldsymbol{E}\right) : (\boldsymbol{d} - \boldsymbol{d}_\theta) + \dot{\boldsymbol{E}} : \boldsymbol{B}_e - \frac{1}{\nu}\left(a^2 \frac{\partial \varphi}{\partial \boldsymbol{T}} : \dot{\boldsymbol{E}} : \boldsymbol{B}_e + \frac{\partial \varphi}{\partial \theta}\,\dot{\theta}\right)\boldsymbol{E} : \boldsymbol{S}\,. \tag{C.10}$$

It should be noted that in case of normal pressures and temperatures $a^2 \approx 1$, $1 + \alpha\theta \approx 1$, and in case of small rotations $\boldsymbol{W} \approx 0$ and $\overset{\nabla}{\boldsymbol{T}} = \dot{\boldsymbol{T}}$, and then Eq. (C.10) and their derivation coincide fully with those in case of small strains.

It should be noted that when calculating $\dot{\boldsymbol{E}}(I_1(\boldsymbol{B}_e), \theta)$ value the relationship

$$\dot{I}_1(\boldsymbol{B}_e) = \boldsymbol{I} : \dot{\boldsymbol{B}}_e = \boldsymbol{I} : \overset{\nabla}{\boldsymbol{B}}_e = a^2(I_1(\boldsymbol{d}) - I_1(\boldsymbol{d}_\theta)) \tag{C.11}$$

was used which follows from Eq. (C.8) and the relation $I_1(\boldsymbol{d}_p) = 0$. When no plastic deformation present $\boldsymbol{d}_p = 0$, the relation (C.10) (the thermoelastic law in terms of rates) is written as follow

$$\overset{\nabla}{\boldsymbol{T}} = a^2 \boldsymbol{E} : (\boldsymbol{d} - \boldsymbol{d}_\theta) + \dot{\boldsymbol{E}} : \boldsymbol{B}_e\,, \tag{C.12}$$

which follows directly from Eqs. (C.3) and (C.8).

Appendix D. Derivation of a tangent stiffness matrix at large strains

The principle of virtual work in a deformed configuration at an arbitrary instant time t is written in the form

$$\int_V \boldsymbol{T} : \boldsymbol{d}^*\, \mathrm{d}V = \int_S \boldsymbol{t} \cdot \boldsymbol{u}^*\, \mathrm{d}V + \int_V \rho \boldsymbol{f} \cdot \boldsymbol{u}^*\, \mathrm{d}V\,, \tag{D.1}$$

where $\boldsymbol{T}$ are Cauchy stress tensors, $\boldsymbol{t}$, $\boldsymbol{f}$ are the specified surface tractions and body forces, $\boldsymbol{u}^*$ are the virtual displacements, $\boldsymbol{d}^* = (\partial \boldsymbol{u}^* / \partial \boldsymbol{x})_s$, ρ is the density, $(\ldots)_s$ designates a symmetrical part of the tensor; V, S are the volume and surface of a body in a deformed configuration; $\boldsymbol{x}$ is the position vector of a point at an instant of time t. With respect to an arbitrary initial configuration at an instant of time t_0 Eq. (D.1) takes the form

$$\int_{V_0} \boldsymbol{T} : \left(\frac{\partial \boldsymbol{u}^*}{\partial \boldsymbol{X}}\right)_s \cdot \frac{\partial \boldsymbol{X}}{\partial \boldsymbol{x}} \frac{\mathrm{d}V}{\mathrm{d}V_0}\, \mathrm{d}V_0 = \int_{S_0} \boldsymbol{t} \cdot \boldsymbol{u}^* \frac{\mathrm{d}S}{\mathrm{d}S_0}\, \mathrm{d}S_0 + \int_{V_0} \boldsymbol{f} \cdot \boldsymbol{u}^* \rho_0\, \mathrm{d}V_0\,, \tag{D.2}$$

where $\boldsymbol{X}$ is the position vector of a point at an instant of time t_0, index '0' designates a quantity value in an initial configuration at an instant of time t_0. To express the principle (D.1) in terms of rates for a deformed configuration we should differentiate Eq. (D.2) in time-independent initial configuration at an instant of time t_0, and then we again pass to a deformed configuration at an instant of time t. Differentiate Eq. (D.2).

$$\int_{V_0}\left(\frac{\partial \dot{\boldsymbol{u}}^*}{\partial \boldsymbol{X}}\right)_s:\left(\frac{\partial \boldsymbol{X}}{\partial \boldsymbol{x}}\cdot \boldsymbol{T}\frac{\mathrm{d}V}{\mathrm{d}V_0}\right)\mathrm{d}V_0+\int_{V_0}\left(\frac{\partial \boldsymbol{u}^*}{\partial \boldsymbol{X}}\right)_s:\overline{\left(\frac{\partial \boldsymbol{X}}{\partial \boldsymbol{x}}\cdot \boldsymbol{T}\frac{\mathrm{d}V}{\mathrm{d}V_0}\right)}^{\boldsymbol{\cdot}}\mathrm{d}V_0$$
$$=\int_{S_0}\dot{\boldsymbol{u}}^*\cdot\left(\boldsymbol{t}\frac{\mathrm{d}S}{\mathrm{d}S_0}\right)\mathrm{d}S_0+\int_{S_0}\boldsymbol{u}^*\cdot\overline{\left(\boldsymbol{t}\frac{\mathrm{d}S}{\mathrm{d}S_0}\right)}^{\boldsymbol{\cdot}}\mathrm{d}S_0+\int_{V_0}\dot{\boldsymbol{u}}^*\cdot\boldsymbol{f}\rho_0\,\mathrm{d}V_0+\int_{V_0}\boldsymbol{u}^*\cdot\dot{\boldsymbol{f}}\rho_0\,\mathrm{d}V_0\,. \tag{D.3}$$

As $\dot{\boldsymbol{u}}^*$ are arbitrary and taking account of Eq. (D.2), it follows that the first, the third and the fifth terms in Eq. (D.3) are canceled. Then

$$\int_{V_0}\left(\frac{\partial \boldsymbol{u}^*}{\partial \boldsymbol{X}}\right)_s\cdot\overline{\left(\frac{\partial \boldsymbol{X}}{\partial \boldsymbol{x}}\cdot \boldsymbol{T}\frac{\mathrm{d}V}{\mathrm{d}V_0}\right)}^{\boldsymbol{\cdot}}\mathrm{d}V_0=\int_{S_0}\boldsymbol{u}^*\cdot\overline{\left(\boldsymbol{t}\frac{\mathrm{d}S}{\mathrm{d}S_0}\right)}^{\boldsymbol{\cdot}}\mathrm{d}S_0+\int_{V_0}\boldsymbol{u}^*\cdot\dot{\boldsymbol{f}}\rho_0\,\mathrm{d}V_0\,. \tag{D.4}$$

Rewrite Eq. (D.4) for a deformed configuration at an instant of time t

$$\int_{V}\left(\frac{\partial \boldsymbol{u}^*}{\partial \boldsymbol{x}}\right)_s\cdot\frac{\partial \boldsymbol{x}}{\partial \boldsymbol{X}}:\overline{\left(\frac{\partial \boldsymbol{X}}{\partial \boldsymbol{x}}\cdot \boldsymbol{T}\frac{\mathrm{d}V}{\mathrm{d}V_0}\right)}^{\boldsymbol{\cdot}}\frac{\mathrm{d}V_0}{\mathrm{d}V}\mathrm{d}V=\int_{S}\boldsymbol{u}^*\cdot\overline{\left(\boldsymbol{t}\frac{\mathrm{d}S}{\mathrm{d}S_0}\right)}^{\boldsymbol{\cdot}}\frac{\mathrm{d}S_0}{\mathrm{d}S}\mathrm{d}S+\int_{V}\boldsymbol{u}^*\cdot\dot{\boldsymbol{f}}\rho\,\mathrm{d}V\,. \tag{D.5}$$

Let $\boldsymbol{F}=\partial\boldsymbol{x}/\partial\boldsymbol{X}$ be a deformation gradient and $\boldsymbol{G}=\boldsymbol{F}^{\mathrm{t}}\cdot\boldsymbol{F}$ be the right Cauchy–Green tensor of deformation. Then, $\mathrm{d}V/\mathrm{d}V_0=\sqrt{I_3(\boldsymbol{G})}$, where $I_3(\boldsymbol{G})$ is the third invariant of the tensor $\boldsymbol{G}$ [35].

Let us consider the subintegral expression in the left-hand part of Eq. (D.5).

$$\left(\frac{\partial \boldsymbol{u}^*}{\partial \boldsymbol{x}}\right)_s\cdot\frac{\partial \boldsymbol{x}}{\partial \boldsymbol{X}}:\overline{\left(\frac{\partial \boldsymbol{X}}{\partial \boldsymbol{x}}\cdot \boldsymbol{T}\frac{\mathrm{d}V}{\mathrm{d}V_0}\right)}^{\boldsymbol{\cdot}}\frac{\mathrm{d}V_0}{\mathrm{d}V}$$
$$=\left(\frac{\partial \boldsymbol{u}^*}{\partial \boldsymbol{x}}\right)_s:\boldsymbol{F}\cdot\left(\dot{\boldsymbol{F}}^{-1}\cdot\boldsymbol{T}\sqrt{I_3(\boldsymbol{G})}+\boldsymbol{F}^{-1}\cdot\dot{\boldsymbol{T}}\sqrt{I_3(\boldsymbol{G})}+\boldsymbol{F}^{-1}\cdot\boldsymbol{T}\cdot\overline{\sqrt{I_3(\boldsymbol{G})}}^{\boldsymbol{\cdot}}\right)\frac{1}{\sqrt{I_3(\boldsymbol{G})}}$$
$$=\left(\frac{\partial \boldsymbol{u}^*}{\partial \boldsymbol{x}}\right)_s:\left(\boldsymbol{F}\cdot\dot{\boldsymbol{F}}^{-1}\cdot\boldsymbol{T}+\dot{\boldsymbol{T}}+\boldsymbol{T}\frac{\overline{\sqrt{I_3(\boldsymbol{G})}}^{\boldsymbol{\cdot}}}{\sqrt{I_3(\boldsymbol{G})}}\right). \tag{D.6}$$

Then, we note that $\dot{\boldsymbol{F}}^{-1}=\boldsymbol{F}^{-1}\cdot\dot{\boldsymbol{F}}\cdot\boldsymbol{F}^{-1}$ (which follows from the differentiation of the relation $\boldsymbol{F}\cdot\boldsymbol{F}^{-1}=\boldsymbol{I}$, where $\boldsymbol{I}$ is the unit tensor), and that $\overline{\sqrt{I_3(\boldsymbol{G})}}^{\boldsymbol{\cdot}}/\sqrt{I_3(\boldsymbol{G})}=\boldsymbol{I}:\partial\boldsymbol{v}/\partial\boldsymbol{X}$, where $\boldsymbol{v}=\dot{\boldsymbol{x}}$ is the velocity [35].

As the choice of an initial configuration is arbitrary, we take $t=t_0$. Then, $\boldsymbol{F}=\boldsymbol{I}$ unit tensor and Eq. (D.6) takes the form

$$\left(\frac{\partial \boldsymbol{u}^*}{\partial \boldsymbol{x}}\right)_s:\left(-\frac{\partial \boldsymbol{v}}{\partial \boldsymbol{x}}\cdot\boldsymbol{T}+\dot{\boldsymbol{T}}+\left(\boldsymbol{I}:\frac{\partial \boldsymbol{v}}{\partial \boldsymbol{x}}\right)\boldsymbol{T}\right). \tag{D.7}$$

Now we consider the first expression in the right-hand part of Eq. (D.5). Taking into account that

$$\overline{\left(\frac{\mathrm{d}S}{\mathrm{d}S_0}\right)}^{\boldsymbol{\cdot}}=\frac{\mathrm{d}S}{\mathrm{d}S_0}\left(\boldsymbol{I}:\frac{\partial \boldsymbol{v}}{\partial \boldsymbol{x}}-\boldsymbol{N}\cdot\boldsymbol{d}\cdot\boldsymbol{N}\right), \tag{D.8}$$

where $\boldsymbol{d}=\frac{1}{2}[\partial\boldsymbol{v}/\partial\boldsymbol{x}+(\partial\boldsymbol{v}/\partial\boldsymbol{x})^{\mathrm{t}}]=(\partial\boldsymbol{v}/\partial\boldsymbol{x})_s$, $\boldsymbol{N}$ is the unit normal to the surface $\mathrm{d}S$ [35], one can obtain

$$\int_{S}\boldsymbol{u}^*\cdot\overline{\left(\boldsymbol{t}\frac{\mathrm{d}S}{\mathrm{d}S_0}\right)}^{\boldsymbol{\cdot}}\frac{\mathrm{d}S_0}{\mathrm{d}S}\mathrm{d}S=\int_{S}\boldsymbol{u}^*\cdot\left[\dot{\boldsymbol{t}}\frac{\mathrm{d}S}{\mathrm{d}S_0}+\boldsymbol{t}\overline{\left(\frac{\mathrm{d}S}{\mathrm{d}S_0}\right)}^{\boldsymbol{\cdot}}\right]\frac{\mathrm{d}S_0}{\mathrm{d}S}\mathrm{d}S$$
$$=\int_{S}\boldsymbol{u}^*\cdot\left[\dot{\boldsymbol{t}}+\boldsymbol{t}\left(\boldsymbol{I}:\frac{\partial \boldsymbol{v}}{\partial \boldsymbol{x}}-\boldsymbol{N}\cdot\boldsymbol{d}\cdot\boldsymbol{N}\right)\right]\mathrm{d}S\,. \tag{D.9}$$

Thus, the final form of the principle of virtual work in terms of rates (D.5) is as follows

$$\int_{V}\left(\frac{\partial \boldsymbol{u}^*}{\partial \boldsymbol{x}}\right)_s:\left(-\frac{\partial \boldsymbol{v}}{\partial \boldsymbol{x}}\cdot\boldsymbol{T}+\dot{\boldsymbol{T}}+\left(\boldsymbol{I}:\frac{\partial \boldsymbol{v}}{\partial \boldsymbol{x}}\right)\boldsymbol{T}\right)\mathrm{d}V+\int_{S}\boldsymbol{u}^*\cdot\left[\dot{\boldsymbol{t}}+\boldsymbol{t}\left(\boldsymbol{I}:\frac{\partial \boldsymbol{v}}{\partial \boldsymbol{x}}-\boldsymbol{N}\cdot\boldsymbol{d}\cdot\boldsymbol{N}\right)\right]\mathrm{d}S+\int_{V}\boldsymbol{u}^*\cdot\rho\dot{\boldsymbol{f}}\,\mathrm{d}V\,. \tag{D.10}$$

Taking into account that the constitutive relations are formulated in form (16) or, which is just the same,

$$\overset{\nabla}{T} = M^1 : d + M^2 \dot{\theta}$$

(where M^1 and M^2 are, respectively, the fourth- and the second-order tensors), Eq. (D.10) can be rewritten as follows

$$\int_V \left(\frac{\partial u^*}{\partial x}\right)_s : \left(-\frac{\partial v}{\partial x} \cdot T + M^1 : d - 2(T \cdot W)_s + \left(I : \frac{\partial v}{\partial x}\right) T\right) \mathrm{d}V - \int_S u^* \cdot t \left(I : \frac{\partial v}{\partial x} - N \cdot d \cdot N\right) \mathrm{d}S$$
$$= \int_S u^* \cdot \dot{t}\, \mathrm{d}S + \int_V u^* \cdot \rho \dot{f}\, \mathrm{d}V - \int_V \left(\frac{\partial u^*}{\partial x}\right)_s : M^2 \dot{\theta}\, \mathrm{d}V\,. \tag{D.11}$$

In terms of indices, Eq. (D.11) can be rewritten as follows

$$\int_V \frac{1}{2}\left(\frac{\partial u_i^*}{\partial x_j} + \frac{\partial u_j^*}{\partial x_i}\right)\left[-\frac{\partial v_j}{\partial x_k} T_{ki} + M^1_{jimn} d_{nm} - (T_{jm} W_{mi} + W^{\mathrm{t}}_{jm} T_{mi}) + \frac{\partial v_m}{\partial x_m} T_{ji}\right] \mathrm{d}V$$
$$- \int_S u_i^* t_i \left(\frac{\partial v_m}{\partial x_m} - N_m \cdot d_{mk} N_k\right) \mathrm{d}S = \int_S u_i^* \dot{t}_i\, \mathrm{d}S + \int_V u_i^* \rho \dot{f}_i\, \mathrm{d}V$$
$$- \int_V \frac{1}{2}\left(\frac{\partial u_i^*}{\partial x_j} + \frac{\partial u_j^*}{\partial x_i}\right) M^2_{ji} \dot{\theta}\, \mathrm{d}V\,. \tag{D.12}$$

Let us introduce index notations of tensors in the rectangular Cartesian coordinates system and standard FE approximations

$$u_i^* = \Psi_{i\beta}(x_m) \bar{u}_\beta^*\,, \qquad v_i = \Psi_{i\alpha}(x_m) \bar{v}_\alpha\,,$$
$$d_{ij} = \frac{1}{2}\left(\frac{\partial \Psi_{i\alpha}}{\partial x_j} + \frac{\partial \Psi_{j\alpha}}{\partial x_i}\right) \bar{v}_\alpha\,, \qquad W_{ij} = \frac{1}{2}\left(\frac{\partial \Psi_{i\alpha}}{\partial x_j} - \frac{\partial \Psi_{j\alpha}}{\partial x_i}\right) \bar{v}_\alpha\,,$$

where $\Psi_{i\alpha}(x_m)$ are the known interpolation functions, u_β^*, v_α are the nodal values of components of the virtual displacement vector and velocity vectors; i, j, $m = \; = 1, 2, 3$; α, $\beta = 1, 2, \ldots, 3 \times M$, M is the number of nodes. Then, Eq. (D.12) can be rewritten as follows

$$\Bigg[\int_V \frac{1}{2}\left(\frac{\partial \Psi_{i\beta}}{\partial x_j} + \frac{\partial \Psi_{j\beta}}{\partial x_i}\right)\Bigg[-\frac{\partial \Psi_{j\alpha}}{\partial x_k} T_{ki} + \frac{1}{2} M^1_{jimn}\left(\frac{\partial \Psi_{m\alpha}}{\partial x_n} + \frac{\partial \Psi_{n\alpha}}{\partial x_m}\right)$$
$$- \frac{1}{2} T_{jm}\left(\frac{\partial \Psi_{m\alpha}}{\partial x_i} - \frac{\partial \Psi_{i\alpha}}{\partial x_m}\right) - \frac{1}{2} T_{mi}\left(\frac{\partial \Psi_{m\alpha}}{\partial x_j} - \frac{\partial \Psi_{j\alpha}}{\partial x_m}\right) + \frac{\partial \Psi_{m\alpha}}{\partial x_m} T_{ij}\Bigg) \mathrm{d}V$$
$$- \int_S \Psi_{i\beta} t_i \left[\frac{\partial \Psi_{m\alpha}}{\partial x_m} - \frac{1}{2} N_m \left(\frac{\partial \Psi_{m\alpha}}{\partial x_k} + \frac{\partial \Psi_{k\alpha}}{\partial x_m}\right) N_k\right] \mathrm{d}S\Bigg] \bar{v}_\alpha$$
$$= \int_S \Psi_{i\beta} \dot{t}_i\, \mathrm{d}S + \int_V \rho \Psi_{i\beta} \dot{f}_i\, \mathrm{d}V - \int_V \frac{1}{2}\left(\frac{\partial \Psi_{i\beta}}{\partial x_j} + \frac{\partial \Psi_{j\beta}}{\partial x_i}\right) M^2_{ji} \dot{\theta}\, \mathrm{d}V\,. \tag{D.13}$$

Eq. (D.13) can be shortly written as follows

$$[K_{\beta\alpha}] \bar{v}_\alpha = \dot{q}_\beta\,, \qquad [K_{\beta\alpha}] = [K^1_{\beta\alpha}] + [K^2_{\beta\alpha}] + [K^3_{\beta\alpha}]\,, \tag{D.14}$$

where

$$[K^1_{\beta\alpha}] = \int_V \underbrace{\frac{1}{2}\left(\frac{\partial \Psi_{i\beta}}{\partial x_j} + \frac{\partial \Psi_{j\beta}}{\partial x_i}\right)}_{[B]^{\mathrm{t}}} M^1_{jimn} \underbrace{\frac{1}{2}\left(\frac{\partial \Psi_{m\alpha}}{\partial x_n} + \frac{\partial \Psi_{n\alpha}}{\partial x_m}\right)}_{[B]} \mathrm{d}V = \int_V [B]^{\mathrm{t}} [M^1][B]\, \mathrm{d}V \tag{D.15}$$

is the conventional tangent matrix which is calculated in the same way as in case of small strains ($[B]$ is the standard kinematic matrix, written in a current configuration),

$$[K^2_{\beta\alpha}] = \int_V \frac{1}{2}\left(\frac{\partial\Psi_{i\beta}}{\partial x_j} + \frac{\partial\Psi_{j\beta}}{\partial x_i}\right)\left[-\frac{\partial\Psi_{j\alpha}}{\partial x_k}T_{ki} - \frac{1}{2}T_{jm}\left(\frac{\partial\Psi_{m\alpha}}{\partial x_i} - \frac{\partial\Psi_{i\alpha}}{\partial x_m}\right)\right.$$
$$\left. - \frac{1}{2}T_{mi}\left(\frac{\partial\Psi_{m\alpha}}{\partial x_j} - \frac{\partial\Psi_{j\alpha}}{\partial x_m}\right) + \frac{\partial\Psi_{m\alpha}}{\partial x_m}T_{ij}\right] \mathrm{d}V\,, \tag{D.16}$$

$$[K^3_{\beta\alpha}] = -\int_S \Psi_{i\beta}t_i\left[\frac{\partial\Psi_{m\alpha}}{\partial x_m} - \frac{1}{2}N_m\left(\frac{\partial\Psi_{m\alpha}}{\partial x_k} + \frac{\partial\Psi_{k\alpha}}{\partial x_m}\right)N_k\right]\mathrm{d}S\,, \tag{D.17}$$

$$\dot{q}_\beta = \int_S \Psi_{i\beta}\dot{t}_i\,\mathrm{d}S + \int_V \rho\Psi_{i\beta}\dot{f}_i\,\mathrm{d}V - \int_V \frac{1}{2}\left(\frac{\partial\Psi_{i\beta}}{\partial x_j} + \frac{\partial\Psi_{j\beta}}{\partial x_i}\right)M^2_{ji}\dot{\theta}\,\mathrm{d}V\,. \tag{D.18}$$

Thus, Eq. (D.14) is the required equation of FEM at large strains, which is written using the tangent stiffness matrix $[K_{\alpha\beta}]$.

Appendix E. Transformation of finite-element equations for solving contact problem

Let us show in what way we can pass from $\{\Delta\bar{u}\}$, $\{\Delta q\}$ vectors in Eq. (43) to $\{\Delta u'\}$ and $\{\Delta q'\}$, in which for contact nodes there stand displacements and a load vector in a local coordinate system (at the rest of the nodes—in a global system), the symmetry of the stiffness matrix $[K]$ being preserved. The transition from the global coordinate system $\boldsymbol{x}_1, \boldsymbol{x}_2, \boldsymbol{x}_3$ to the local coordinate system $\boldsymbol{r}_i, \boldsymbol{r}_j, \boldsymbol{r}_n$ is realized by the rotation matrix $[z]$: $\{\boldsymbol{r}_i, \boldsymbol{r}_j, \boldsymbol{r}_n\}^{\mathrm{t}} = [z]\{\boldsymbol{x}_1, \boldsymbol{x}_2, \boldsymbol{x}_3\}^{\mathrm{t}}$. Then, $\{\Delta\bar{u}\} = [\alpha]\{\Delta u'\}$; $\{\Delta q\} = [\alpha]\{\Delta q'\}$. Matrix $[\alpha]$ has the following structure

$$[\alpha] = \begin{bmatrix} 1 & & 0 \\ & [z_m] & \\ 0 & & 1 \end{bmatrix}. \tag{E.1}$$

There are rotation matrices $[z_m]$ $(m = 1, 2, \ldots M$; where M is the number of pairs of the contact nodes) in the main diagonal of the matrix $[\alpha]$ for contact nodes. There are unities in the main diagonal of the matrix for non-contact nodes; the rest elements of the matrix $[\alpha]$ are zero; $[\alpha]^{\mathrm{t}}[\alpha] = [I]$ is the unit matrix. Substituting $\{\Delta\bar{u}\}$ and $\{\Delta q\}$ into (43), we have

$$[K']\{\Delta u'\} = \{\Delta q'\}\,, \tag{E.2}$$

where $[K'] = [\alpha]^{\mathrm{t}}[K][\alpha]$ is the symmetric matrix. For the nodes in contact, the components of $\{\Delta q'\}$ are unknown but there must be satisfied the relations $(38)_2$, (42) and (44).

Now we show that to satisfy the relations $(38)_2$, (42) and (44) (similarly to the transition from the global coordinate system to the local one) the matrix $[\beta]$ can be used which rotates the elements of $\{\Delta u'\}$ and $\{\Delta q'\}$ vectors with components $\{\Delta\bar{u}^A_p, \Delta\bar{u}^B_p\}$, $\{\Delta q^A_p, \Delta q^B_p\}$, $p = i, j, n$ through 45°. Thus, we changeover from the system (E.2) to the system

$$[\tilde{K}]\{\Delta\tilde{u}\} = \{\Delta\tilde{q}\}\,, \tag{E.3}$$

where $[\tilde{K}] = [\beta]^{\mathrm{t}}[\alpha]^{\mathrm{t}}[K][\alpha][\beta]$ is the symmetric matrix, $\{\Delta\tilde{u}\} = [\beta]\{\Delta u'\} = [\beta][\alpha]\{\Delta\bar{u}\}$, $\{\Delta\tilde{q}\} = [\beta]\{\Delta q'\} = [\beta][\alpha]\{\Delta q\}$. Matrix $[\beta]$ has the following structure

$$[\beta] = \begin{bmatrix} 1 & & & & 0 \\ & \beta_{dd} & & \beta_{dt} & \\ & & 1 & & \\ & \beta_{td} & & \beta_{tt} & \\ 0 & & & & 1 \end{bmatrix}. \tag{E.4}$$

For the matrix $[\beta]$ there are unities in the main diagonal except for the elements $\beta_{dd} = \beta_{tt} = \cos 45°$ and zero beyond the main diagonal except for the elements $\beta_{td} = -\beta_{dt} = -\sin 45°$ (where d and t are the number of mth component of displacement vector of the A and B nodes, respectively, in the total list of elements of the vector $\{\bar{u}\}$; $m = 1, 2, 3$). Thus, the elements of the $\{\Delta\tilde{u}\}$ and $\{\Delta\tilde{q}\}$ vectors for the nodes beyond the contact surface are equal to those of the $\{\Delta\bar{u}\}$ and $\{\Delta q\}$ vectors; for nodes in the contact surfaces

$$\Delta\tilde{u}_p^+ = \frac{\sqrt{2}}{2}(\Delta\bar{u}_p^A + \Delta\bar{u}_p^B)\,; \qquad \tilde{u}_p^- = \frac{\sqrt{2}}{2}(\Delta\bar{u}_p^A - \Delta\bar{u}_p^B)\,; \tag{E.5}$$

$$\Delta\tilde{q}_p^+ = \frac{\sqrt{2}}{2}(\Delta q_p^A + \Delta q_p^B) = \frac{\sqrt{2}}{2}[(\Delta\bar{t}_p^A + \Delta\bar{t}_p^B) + (\Delta\bar{f}_p^A + \Delta\bar{f}_p^B)]\,; \tag{E.6}$$

$$\Delta\tilde{q}_p^- = \frac{\sqrt{2}}{2}(\Delta q_p^A - \Delta q_p^B) = \frac{\sqrt{2}}{2}[(\Delta\bar{t}_p^A - \Delta\bar{t}_p^B) + (\Delta\bar{f}_p^A - \Delta\bar{f}_p^B)]\,; \quad p = n, i, j\,, \tag{E.7}$$

where $\Delta\bar{u}_p$, Δq_p, $\Delta\bar{t}_p$, $\Delta\bar{f}_p$ are the incremental components of the nodal displacement vector, load vector, the load vector due to contact and body forces written in the local coordinate system, respectively; the superscripts A and B correspond to points A and B.

References

[1] V.I. Levitas, Large Deformation of Materials with Complex Rheological Properties at Normal and High Pressure (Nova Science Publishers, New York, 1995).

[2] V.I. Levitas, Large Elastoplastic Deformations of Materials at High Pressure (Naukova Dumka, Kiev, 1987) [in Russian].

[3] J.C. Simo and C. Miehe, Associative coupled thermoplasticity at finite strains: Formulation, numerical analysis and implementation, Comput. Methods Appl. Mech. Engrg. 98 (1992) 41–104.

[4] N. Atluri, On constitutive relations at finite strain: hypoelasticity and elasto-plasticity with isotropic or kinematic hardening, Comput. Methods Appl. Mech. Engrg. 43 (1984) 137–171.

[5] L.B. Freund, Constitutive equations for elastic-plastic materials at finite strain, Int. J. Solids Struct. 6 (1970) 1193–1209.

[6] A.E. Green and P.M. Naghdi, A general theory at an elastic-plastic continuum, Arch. Ration. Mech. Anal. 186 (1965) 251–281.

[7] E.H. Lee, Elastic-plastic deformation at finite strains, Trans. ASME: J. Appl. Mech. 36 (1969) 1–6.

[8] B. Loret, On the effects of plastic rotation in the finite deformation of anisotropic elastoplastic materials, Mech. Mater. 2 (1983) 278–304.

[9] P.M. Naghdi and J.A. Trapp, On finite elastic-plastic deformation of metals, J. Appl. Mech. 41 (1974) 254–260.

[10] S. Nemat-Nasser, Decomposition of strain measures and their rates in finite deformation elasto-plasticity, Int. J. Solids Struct. 15 (1979) 155–166.

[11] F. Sidoroff, Incremental constitutive equation for large strain elasto-plasticity, Int. J. Engrg. Sci. 206 (1982) 19–26.

[12] E. Stein and C. Miehe, Theory and finite element computation of finite elasto-visco-plastic strains, in: J.-P. Boehler and A.S. Khan, eds., Anisotropy and Localization of Plastic Deformation (Elsevier Applied Science, London, 1991) 409–412.

[13] J.H. Cheng and N. Kikuchi, An analysis of metal forming processes using large deformation elastic-plastic formulations, Comput. Methods Appl. Mech. Engrg. 49 (1985) 71–108.

[14] H.D. Hibbit, P.V. Marcal and J.R. Rice, A finite element formulation for problems of large strain and large displacement, Int. J. Solids Struct. 6 (1970) 1069–1086.

[15] R.M. McMeeking and J.R. Rice, Finite-element formulation for problems of large elastic-plastic deformation, Int. J. Solids Struct. 11 (1975) 601–616.

[16] M.S. Gadala, G.A.E. Oravas and M.A. Dokainish, A consistent Eulerian formulation of large deformation problems in statics and dynamics, Int. J. Non-Linear Mech. 18 (1983) 21–35.

[17] M.S. Gadala, M.A. Dokainish and G.A.E. Oravas, Formulation of methods of geometric and material non-linearity problems, Int. J. Numer. Methods Engrg. 20 (1984) 887–914.

[18] K. Mattiasson, On the co-rotational finite element formulation for large deformation problems, Ph.D. Dissertation, Chalmers University of Technology, Goteborg, Sweden, 1983.

[19] A. Chandra and S. Mukhergee, A finite element analysis of metal forming processes with thermomechanical coupling, Int. J. Mech. Sci. 26 (1985) 661–676.

[20] J.H. Argyris and J.St. Doltsinis, On the large strain inelastic analysis in natural formulation—Part I. Quasistatic problems, Comput. Methods Appl. Mech. Engrg. 20 (1979) 213–251.

[21] J.H. Argyris and J.St. Doltsinis, On the natural formulation and analysis of large deformation coupled thermomechanical problems, Comput. Methods Appl. Mech. Engrg. 25 (1981) 195–253.

[22] Y. Yamada, Nonlinear matrices, their implication and applications in in elastic large deformation analysis, Comput. Methods Appl. Mech. Engrg. 33 (1982) 417–437.

[23] J.C. Simo and T.J.R. Hughes, Elastoplasticity and viscoplasticity—Computational aspects, Springer Ser. Appl. Math. (Springer, Berlin, 1989).

[24] B. Fredriksson, Finite element solution of surface non-linearities in structural mechanics with special emphasis to contact and fracture mechanics problems, Comput. Struct. 6 (1976) 281–290.

[25] K.J. Bathe and A. Chaudhary, A solution method for planar and axisymmetric contact problems, Int. J. Numer. Methods Engrg. 21 (1985) 65–88.

[26] B. Jorstenfelt, Contact problems with friction in general purpose finite element computer programs, Comput. Struct. 16 (1983) 487–493.

[27] M. Mazurkiewicz and W. Ostachowicz, Theory of finite element method for elastic contact problems of solid bodies, Comput. Struct. 17 (1983) 51–59.

[28] R. Michalowski and Z. Mroz, Associated and non-associated sliding rules in contact friction problems, Arch. Mech. Stosow. 30 (1978) 259–276.

[29] J.T. Oden and E.B. Pires, Algorithms and numerical results for finite element approximations of contact problems with non-classical friction laws, Comput. Struct. 19 (1984) 137–147.

[30] E.A. Wilson and B. Parsons, Finite element analysis of elastic contact problems using differential displacements, Int. J. Numer. Methods Engrg. 2 (1970) 387–395.

[31] V.I. Levitas and A.V. Idesman, Solving of thermoelastoplastic problems at contact interaction using FEM, Strength of Materials 11 (1986) 77–83.

[32] E.M. Morozov and G.P. Nikishkov, FEM in Fracture Mechanics (Nauka, Moscow, 1980) [in Russian].

[33] V.I. Levitas, A.V. Idesman, A.B. Nemirovsky, et al., Numerical modelling of the process for pressing matrices into a block of rings with regard to plastic deformations and friction forces, Strength of Materials 22 (1990) 1675–1682

[34] N.V. Novikov, V.I. Levitas, S.I. Shestakov, et al., FEM modelling of electrical, temperature fields and thermo-stress fields in HPA, Sverkhtverdye Materialy 3 (1983) 3–8.

[35] A.I. Lurje, Non-linear Theory of Elasticity (Nauka, Moscow, 1980) [in Russian].